

This report is related to the FY2023 Subsidized Project of Decommissioning, Contaminated Water and Treated Water Management (Development of Analysis and Estimation Technology for Characterization of Fuel Debris).

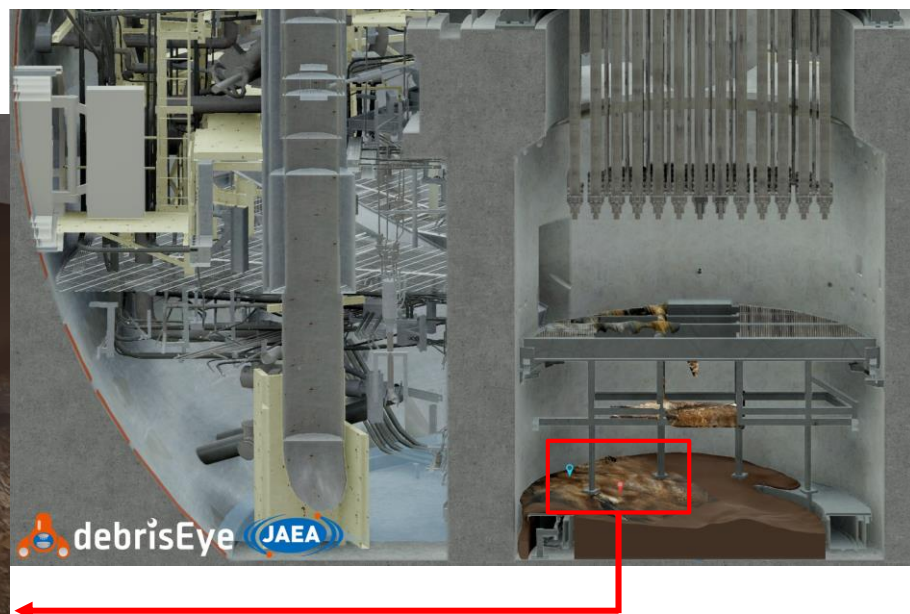
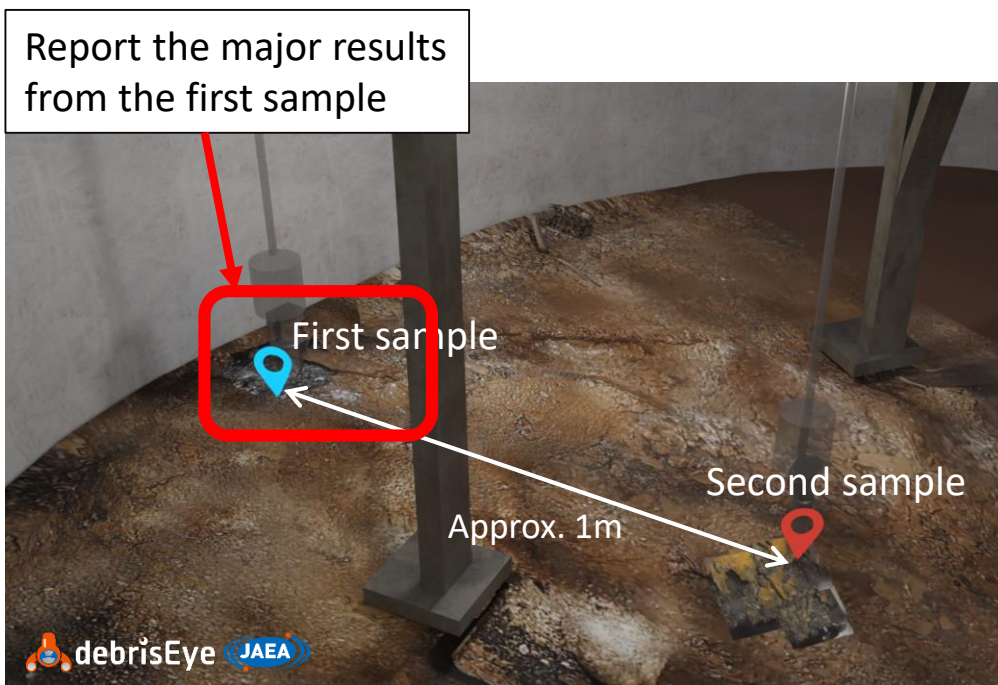
Analysis results of the first fuel debris sample

July 31, 2025

Japan Atomic Energy Agency

Tokyo Electric Power Company Holdings, Inc.

- On November 12, 2024, the first fuel debris sample taken during trial fuel debris retrieval was received at the JAEA Oarai Nuclear Engineering Institute's Irradiated Fuel Monitoring Facility (FMF).
- Non-destructive analysis, fractionation and sample transport were completed by January 2025. We reported this at Decommissioning, Contaminated Water, and Treated Water Countermeasures Team Meeting / Secretariat Meeting on January 30, 2025 (refer to the reference materials).
- At this meeting, a report will be given on the major results of detailed analysis that have been obtained since then.



Fuel debris sampling locations on the floor inside the Unit 2 pedestal

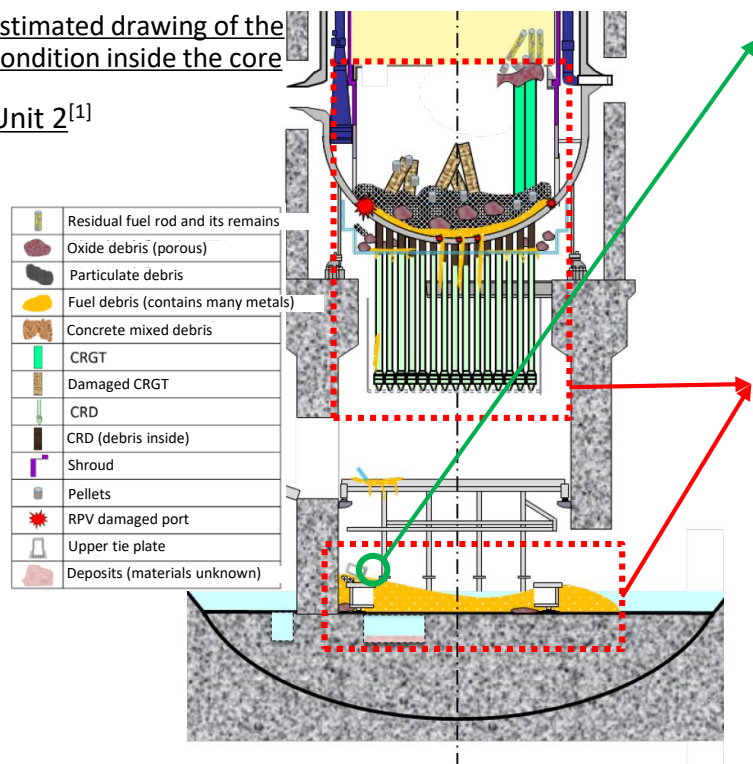
- By analyzing the obtained sample, grasp the condition of the sampled area to estimate the formation process of the fuel debris.
- ⇒ More precise estimation of the condition inside the core will become the basis for review of full-scale fuel debris retrieval to safely retrieve fuel debris and realize thoroughly managed stable storage.

<Example of incorporating “estimation of the condition inside the core” into “review of fuel debris retrieval methods”>

- Estimate hardness of fuel debris → select retrieval methods and tools
- Possibility of criticality of fuel debris → review safety measures and storage methods

Estimated drawing of the condition inside the core

Unit 2^[1]



1. Grasping the condition of the sampled area

(Grasping the condition of the fuel debris sample)

- Acquisition of **information tailored to decommissioning needs**
 - ✓ Grasp the type and concentration of major components (nuclide/element) in the sample and review the origin of each component
 - ✓ Grasp the content and distribution of fuel components in the sample

2. Estimation of formation process of fuel debris

- Estimation of fuel debris properties through **review of in-core environment during the accident**
 - ✓ Estimate the formation conditions of the sample based on microstructure, composition of constituent phases and crystal structure of phases including U in the sample.
 - ✓ Evaluate the surrounding of the sampled area based on the comparison of existing accident scenarios with the internal investigation results (evaluate based on the results of multiple future sample analyses)

[1] JAEA, FY2022 Report of the FY2022 Subsidized Project of Decommissioning, Contaminated Water and Treated Water Management (Development of Analysis and Estimation Technology for Grasping Fuel Debris Properties (Development of Technology for Estimating Damage Conditions of the Reactor Pressure Vessel)).

1. Grasping the condition of the sampled area (Grasping the condition of the fuel debris sample)

Analysis items	Analysis methods	Evaluation details	Examples of major applications for decommissioning
Basic information • External appearance, weight • Dose rate • Density distribution [Previously announced : Reference materials]	• Exterior, weight, dose rate measurement • Imaging plate (IP) • X-ray CT	Organization of basic information	Basic information to review retrieval (existence and mount of pores, etc.)
Element content① (elemental composition)	• ICP-MS, ICP-AES	Content of fuel components Origin of major components	Basic information to review safety measures at retrieval, such as criticality evaluation, and storage methods
Isotope ratio②	• TIMS • SIMS	U isotope ratio	
Element and compound distribution③	• SEM-EDX, SEM-WDX • TEM-EDX • XRD	Evaluation of distribution of elements and compounds (including pores)	Basic information to review retrieval methods and tools (estimation of hardness, toughness, etc.)
Radioactive concentration④	• γ -ray spectrometry • α -ray spectrometry • β -ray spectrometry • Liquid scintillation counter, etc.	Accompanied condition of U with focal nuclides Amount of radioactivity of nuclides targeted for analysis	Information to review technology development for non-destructive measurement at fuel debris retrieval Information needed to deliberate treatment/disposal

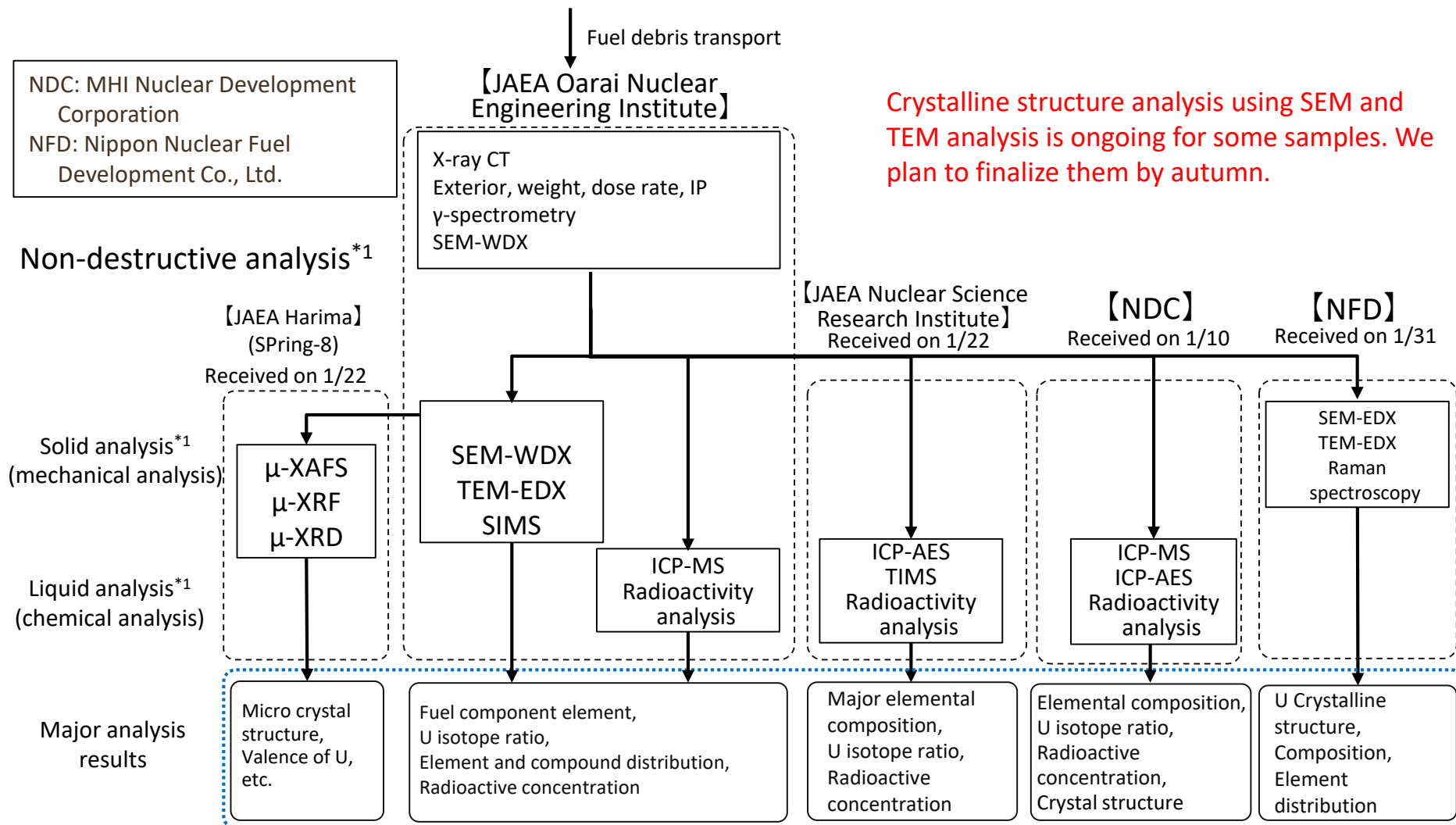
2. Estimation of formation process of fuel debris

Analysis items	Analysis methods	Evaluation details	Examples of major applications for decommissioning
Crystal structure and composition of phases including U⑤	• SEM-EDX, SEM-WDX • TEM-EDX • Raman spectroscopy • XRD • μ -XAFS • μ -XRF • μ -XRD	Estimation of temperature and atmosphere when U particles, etc. are formed Oxidation state of U, etc.	Precise estimated drawing of the condition inside the core to review retrieval methods and internal investigation

See the list of abbreviations at the end of the document for abbreviations of analysis methods

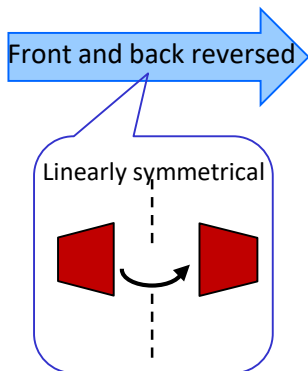
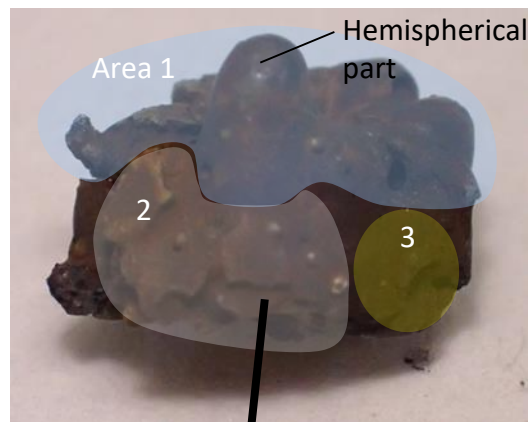
- The major results (solid/liquid analysis) of the detailed analysis are reported below.

【Fukushima Daiichi Nuclear Power Station Unit 2】



*1 Overview and purpose of each analysis are described in the reference documents

External photos of fuel debris samples



Hemispherical part



Approx. 3mm

Area 1



Approx. 7mm

Block, for Oarai Sample [A-1]

Area 2



Block, for NDC Sample [D]



Small particles after being crushed

Block + Particles, for Nuclear Science Research Institute Sample [B]

Area 3



Block, for NFD Sample [C]



Small fragments after crushing

Block + Particles, For Oarai Nuclear Engineering Institute + SPring-8 Sample [A-2]

- The sample was fractionated (hit and crushed with a stainless rod (approx. 250g)) for each analysis institute.

- ◆ In order to identify and quantify the elements contained in the fuel debris [block \[D\]](#) and [particles \[B\]](#) obtained through crushing, the specimens were fractionated, dissolved (approx. 0.1g each specimen), and analyzed.

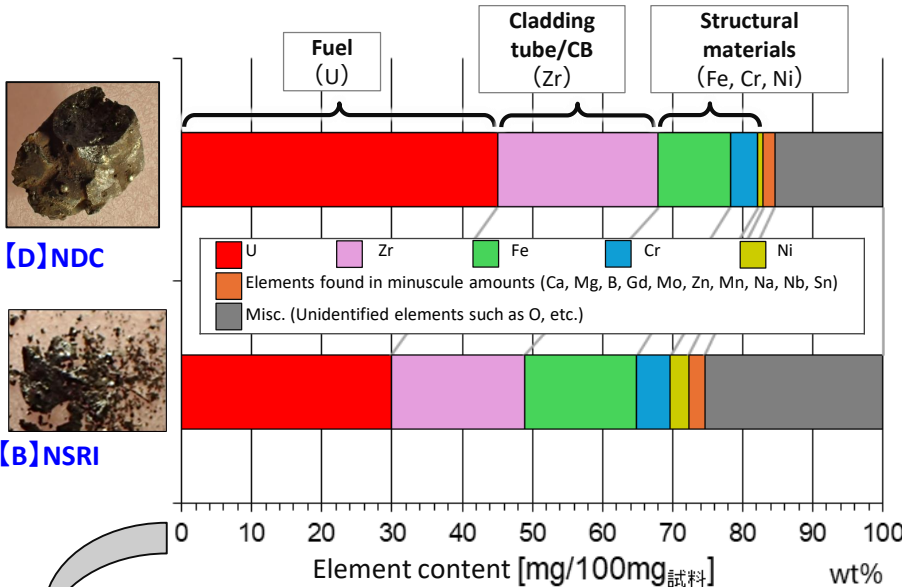


Figure 1 Elemental composition of the sample (ICP-AES and ICP-MS analysis results)

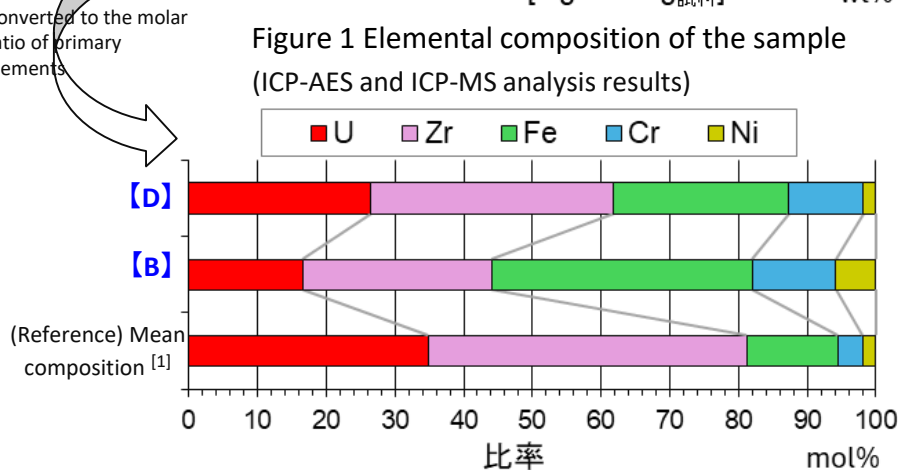


Figure 2 Ratio of major elements (U, Zr, Fe, Cr, Ni)

- U, Zr, Fe, Cr and Ni were the primary elements in all samples. The ratio of U was highest compared to sample mass. (Figure 1)

- The ratio of structural material elements (Fe+Cr +Ni) was higher than the initial mean composition of fuel, cladding tubes/CB, and control rod blades in Unit 2. (Figure 2)

⇒ It is possible that after the fuel and cladding tubes, etc. melted in the core, these elements were generated as other materials got caught up in the molten material as it migrated to the PCV.

- The following elements were also found in minuscule amounts: Ca, Mg, B, Gd, Mo, Zn, Mn, Na, Nb, Sn. (All at amounts less than 1wt% of the sample mass)

⇒ In light of the structural materials inside the PCV and RPV as well as conditions during the accident, it is possible that these elements originate from seawater elements, as well as structural elements and the paint, etc. they were covered with.

- The ratio of fuel elements (uranium) differed in the parts of the sample that remained in block [D] and the parts that were turned to particles [B] during crushing (Figure 2).

⇒ [B] suggests a larger ratio of the micro-mixed phase (Considering ④ Element, compound distribution)

- ◆ In order to ascertain differences, each fractionated sample from [block \[D\]](#) and [particles \[A-2\]\[B\]](#) obtained through crushing were dissolved and TIMS or ICP-MS were used to quantify the uranium isotopes (^{234}U , ^{235}U , ^{236}U and ^{238}U) in the solution.

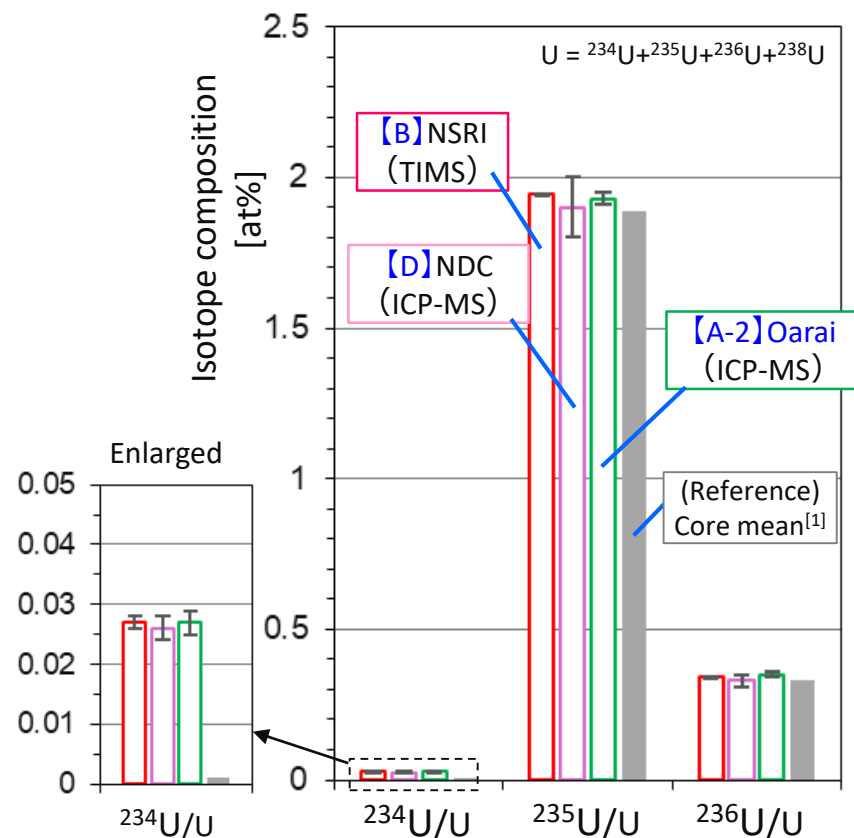


Figure 1 U isotope composition analysis of dissolved solution

- Level of uranium enrichment ($^{235}\text{U}/\text{U}$ ratio)

- $^{235}\text{U}/\text{U}$ ratio was approx. 1.9at% (Approx. 1.9wt%) for all specimens, and it was confirmed that the difference between fractionated specimens is miniscule. (Figure 1)

➤ $^{235}\text{U}/\text{U}$ ratio in the samples was practically the same and close to the core means.

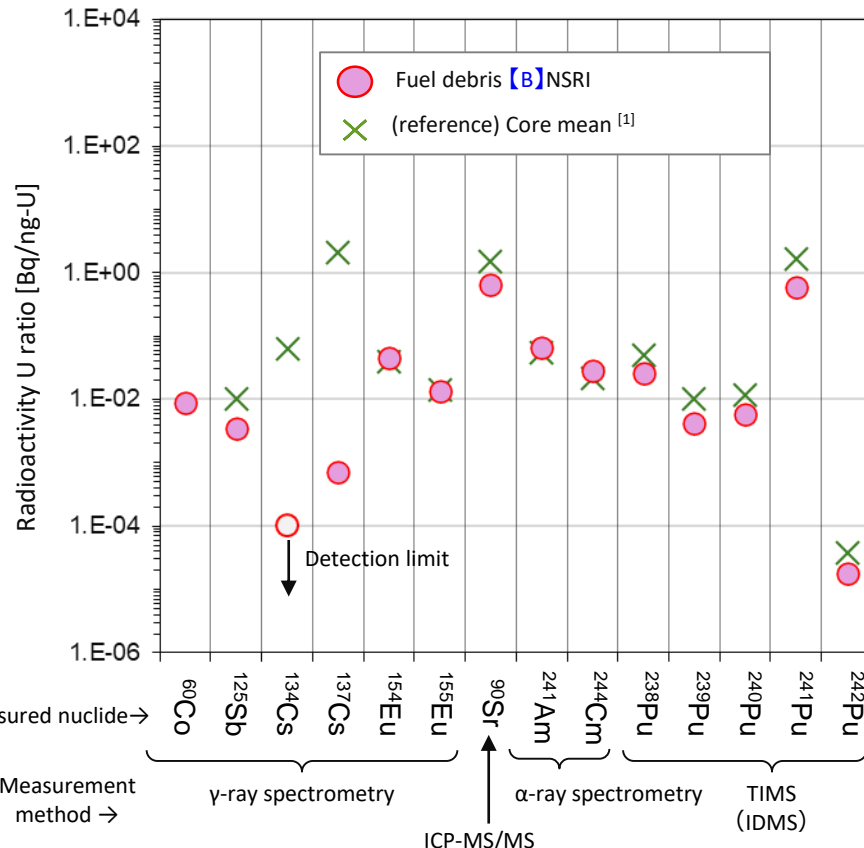
⇒ It is possible that the $^{235}\text{U}/\text{U}$ ratio in the fuel debris equalized to that prior to the accident through the melting/mixing process.

U isotope ratio analysis will be continued to estimate the degree of melting/mixing.

※ $^{235}\text{U}/\text{U}$ ratio distribution in the core prior to the accident was between less than 1% to approx. 4%

A large range of fuel debris samples will need to be analyzed going forward to determine whether or not the level of enrichment indeed equalized throughout all of the fuel debris.

- ◆ In order to ascertain primary radioactive nuclides, fractionated specimens of [particles \[B\]](#) obtained through crushing were dissolved and the concentration of radioactivity in the solution was measured using γ -ray spectrometry and α -ray spectrometry, etc. In order to assess the association with uranium, which is the primary element in fuel, the ratio of nuclide radioactivity to uranium mass was calculated and compared with past samples and core means.



○ Major radioactive nuclides

- ^{90}Sr , α nuclides (^{241}Am , ^{244}Cm , and Pu isotopes), ^{154}Eu and ^{60}Co contribute greatly to the radioactivity in fuel debris samples. (Left figure)
- The contribution of ^{134}Cs and ^{137}Cs is small, and less than core means.

⇒ It is possible that during the accident, radioactive Cs volatilized due to the high temperatures and formed fuel debris with low γ dose rates.

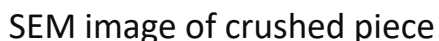
○ Accompanied condition of U

- The ratio of Sr, Eu, Pu, Am, Cm to U is very similar to core means.

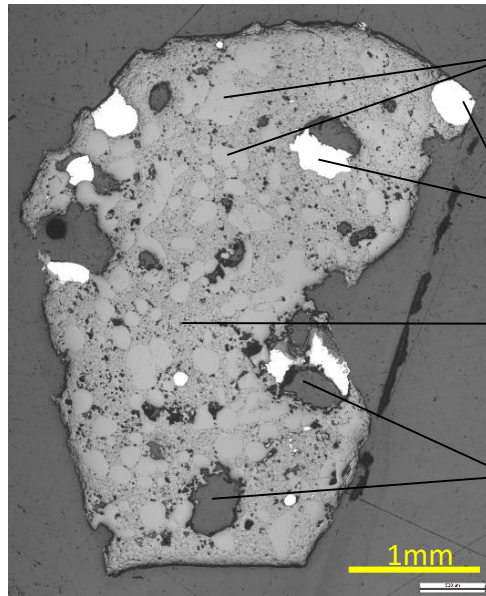
⇒ ^{154}Eu and ^{244}Cm , which are searched ※ for to detect fuel debris, were found to associate with U.

※ Because they are known to associate with U after normal nuclear reactor operation.

⇒ It is possible that small amounts were caught up in the seawater, thermal layer, and paint, etc.



【C】 NFD



External appearance of cut face
※ Sample sliced (refer to the reference materials for information on the cut face)

Optical microscope image of cut face

External appearance and optical microscope image of cut face

Area ratio of each region[%]

(A)Zr-U-O	(B)Fe-Ni	(C)Micro-phase	(D)Pore
20	4.4	56	19

[Constituent phases classification/summary]

※ The elements contained in each phase are based on SEM-EDX analysis results

(A)Zr-U-O phase (Several tens ~ Several hundreds μm)

- Zr/U atomic ratio is approx. 2 (Almost constant regardless of grain)

(B)Fe-Ni metal phase (Several tens ~ Several hundreds μm)

- Fe/Ni atomic ratio is approx. 1~3 (Differs according to grain)

(C) Micro-mixed phase

- U-Zr-O, Zr-U-O, Fe-Cr-O, Fe-O mixed phase

(D)Pores (Several tens ~ Several hundreds μm)

- Approx. 20% of the area of the cut face

⇒ The primary phases that were observed were a Zr-U-O phase, Fe-Ni metal phase, and micro-mixed phase (region of mixed U and oxidized Fe), and the same phases were found on the surface of crushed parts of other areas (refer to page 10).

⇒ A micro-phase that contains small pores was found dispersed throughout the entire sample meaning that it may be able to be crushed relatively easily (considering the difference in the elemental composition of powdered samples noted in ① Elemental Composition)

It is assumed that this sample was easy to crush by hand because it was a mixture of micro-phases and pores. It also did not contain large boride precipitates that have been found to be the hardest phase.

◆ Difference between the surface and the internal parts of fuel debris

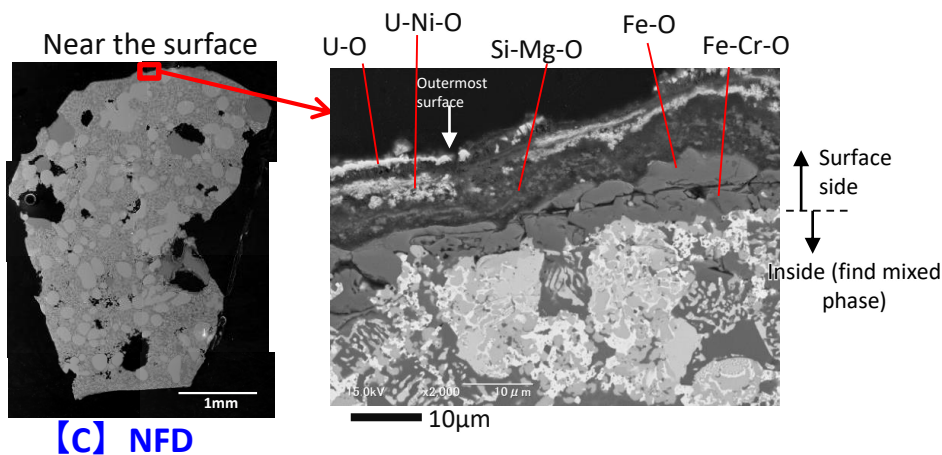
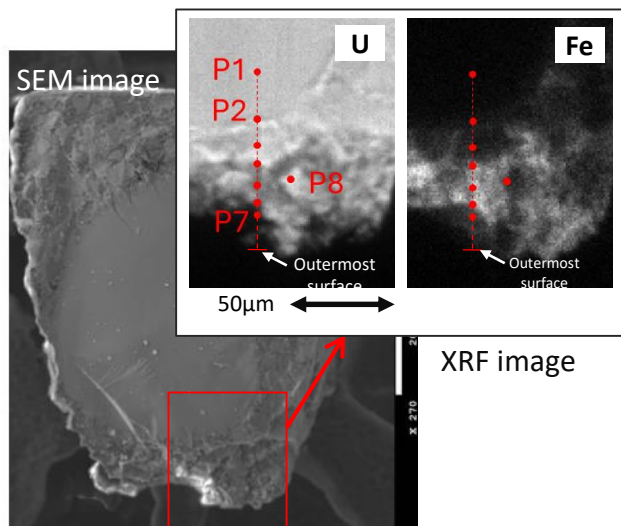


Figure 1 SEM image of near the surface of the fuel debris sample



[A-2] SPring-8

- Observations of the cut face found that the surface of the fuel debris is a layered structure made up of U, Ni, Si, Mg, Fe, Cr, etc. with a different elemental distribution from the inside. (Figure 1)
- Synchrotron analysis of the crushed fragments found a tendency for the valence of U and Fe to increase near the surface. (Figure 2)

⇒ It is assumed that the surface of the fuel debris was more susceptible to oxidization than the inside. TEM will be used to perform further detailed analysis of the crystalline structure near the surface since it may tell us about the environments inside the RPV/PCV after the accident.

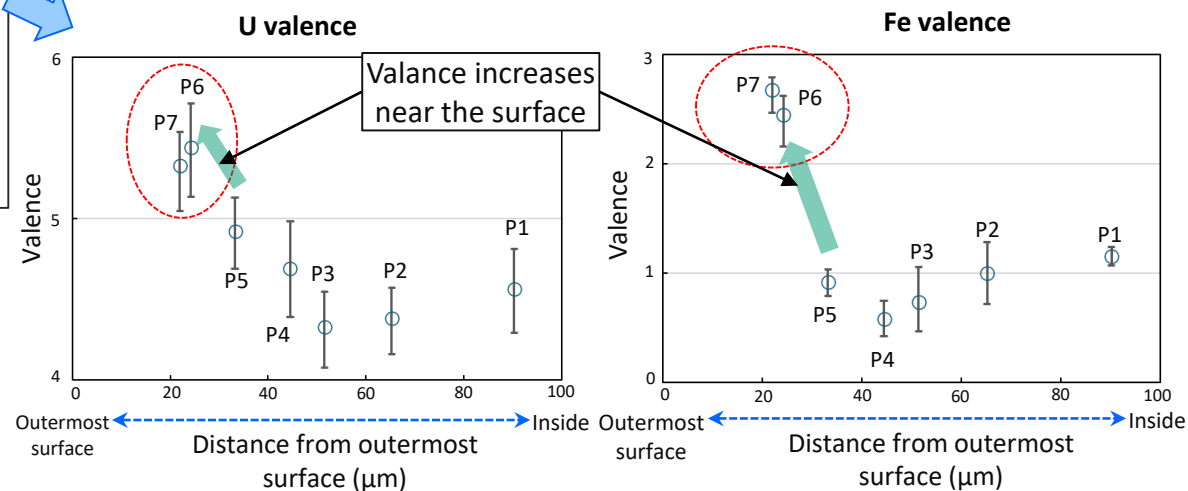


Figure 2 Assessment results of valence near the surface of crushed fuel debris fragments (µ-XAFS results)

Fuel and cladding tubes, etc.
melt in the core

Uranium fuel, zirconium metal and
stainless steel, etc., melt together

→ Zr-U-O phase, U-Zr-O phase, Fe-
Cr-O phase, Fe-O phase, Fe-Ni
phase observed (page 10~11)

Various materials get mixed in as
the molten material migrates and
falls into the PCV

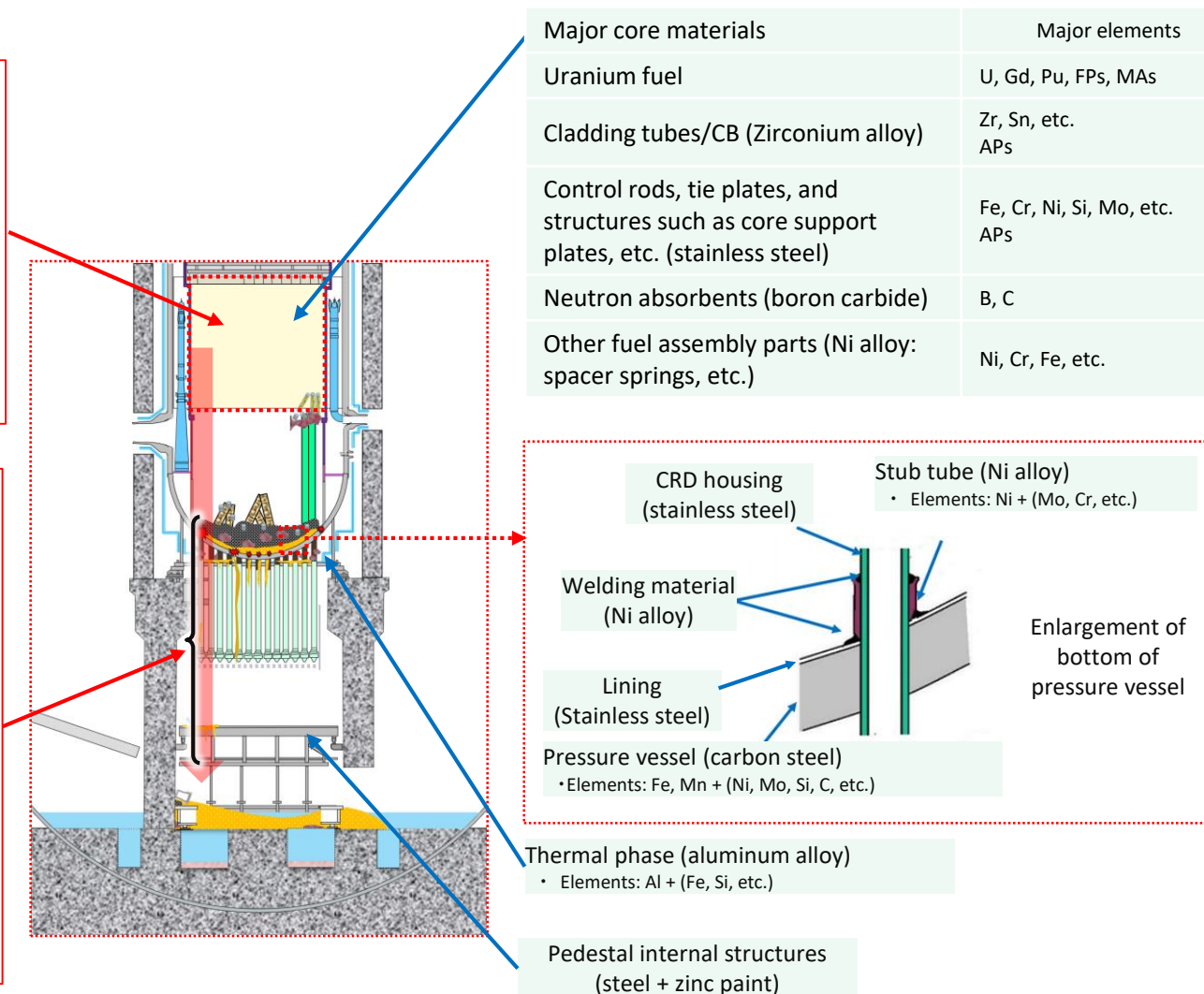
- CRD housing (stainless steel)
- Welding material, stub tubes, (Ni alloy)

→ The percentages of the structural
material elements Fe+Cr+Ni are high
(page 7)

Fe-Ni phase observed (page 11)

- Thermal phase (Al alloy)

→ Al detected (page 10)



Fuel debris analysis results used to provide more detail on the figure thereby estimating conditions inside the core.

- ① Fuel elements (U) were the most abundant relative to the mass of the sample. However, when compared to core composition, the mass of structural material elements (Zr,Fe,Cr,Ni) was larger than fuel elements (U), so it is possible that as the material migrated into the PCV, it mixed with other materials.
 - ② The level of uranium enrichment was approx. 1.9wt% for the ratio of $^{235}\text{U}/\text{U}$, there was no sample bias, and values were close to core means. Fuel debris will be sampled from a wider area and analyzed.
 - ③ In regards to γ -ray emitting nuclides, the concentration of Cs was low, and the concentrations of Eu and Co were high. It is highly possible that radioactive Cs volatilized in the high temperatures during fuel debris creation.
 - ④ The fuel debris is primarily comprised of Zr-U-O phase, Fe-Ni metal phase, a micro-mixed phase and pores. It is assumed that the sample can be crushed relatively easily.
 - ⑤ On the surface of the fuel debris, the uranium valence and crystallinity of the elements as they exist differs from the inside, and suggests that they were subject to an oxidizing environment
- We will continue to generate hypotheses about the conditions inside the reactors at the time of the accident and the process by which fuel debris was created, while also ascertaining the conditions around fuel debris sampling locations (inside the pedestal), and where fuel debris was created (inside the RPV, etc.). To do this, we will continue micro-structure observations and crystalline structure analysis with the intention of compiling a report in this autumn.

- ◆ Valuable data has been obtained from the analysis of a small fuel debris sample, and this knowledge will be leveraged for future fuel debris retrieval.
- ◆ This assessment is based on the analysis results of a small sample, and revisions will be continually made based on knowledge obtained through future analysis.

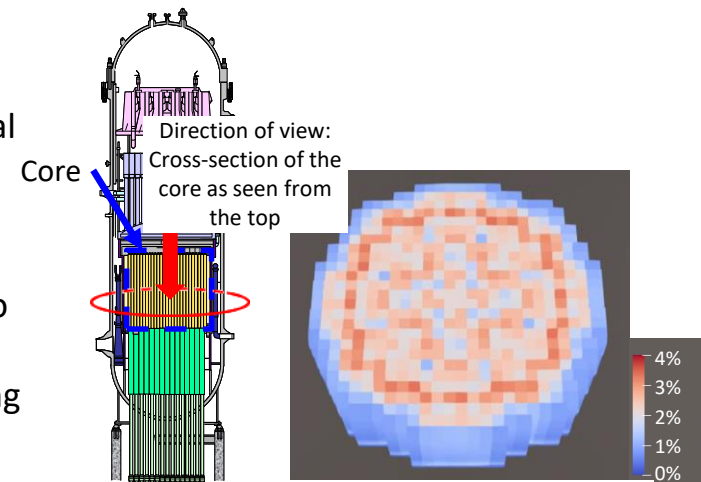
1. Grasping the condition of the sampled area

■ Deliberating safety measures and storage methods during retrieval (Scope of uranium enrichment)

- The level of uranium enrichment was close to core means. Since the level of uranium enrichment in the fuel debris is close to the enrichment distribution in the Unit 2 core prior to the accident (approximately less than 1%~4%), it is possible that the level of enrichment equalized as the fuel mixed during melting and solidification.
- The degree of enrichment is a parameter used to assess criticality when deliberating safety measures and storage methods during retrieval, so if the anticipated degree of enrichment can be reduced based on actual analysis results, then it will be possible to design the retrieval method more logically.

(Radiation sources that should be considered during dose assessments)

- It appears that Cs volatilized in conjunction with the high heat/melting of fuel during the accident, and that the concentration of ^{137}Cs was approximately 1/1,000 that of the core mean (spent fuel).
- However, since there is little ^{137}Cs , the impact of ^{154}Eu and ^{60}Co was relatively large, so this knowledge will be leverages for exposure countermeasures.



Example of enrichment level distribution in the BWR core
(red shows the degree of high enrichment)

- Information used to deliberate the development of non-destructive measurement technologies used during fuel debris retrieval
 - ^{154}Eu and ^{244}Cm , which are difficult to volatilize, are associated with U. By analyzing the amount of ^{154}Eu , ^{244}Cm and U present in actual fuel debris, we have quantitatively confirmed that the association is good.
 - Data pertaining to association can be leveraged to deliberate non-destructive analysis methods such as those that use ^{154}Eu and ^{244}Cm , which emit gamma rays and neutron rays, in lieu of, and to indicate, U, which is relatively difficult to measure, such methods already being developed.
- Basic information for deliberating retrieval methods/tools
 - Observation of cut faces revealed many pores and the fractionated samples could be crushed by hand at analysis facilities.
 - It is assumed that fuel debris with the same structure can be crushed so this information will be used to deliberate processing jigs.

2. Estimation of formation process of fuel debris

- Refining hypotheses about conditions inside the reactors will help to deliberate retrieval methods and internal investigations
 - It is assumed that fuel and cladding tubes, etc. melted inside the core and mixed with other materials as the molten material migrated to the floor the pedestal.
 - We will continue to analyze the crystalline structure of phases containing uranium, etc., with the intent of obtaining data that will be useful for hypothesizing temperatures and atmospheric conditions during fuel debris creation.
 - By mixing this information with data obtained to date, we will continue to hypothesize how the accident unfolded, and strive to ascertain conditions inside the reactor, such as fuel debris distribution, etc., with the intention of leveraging this information to deliberate fuel debris retrieval methods and internal investigations.

Reference Materials

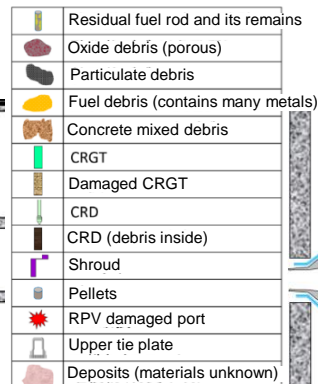
- Materials that might have been caught up in the creation process of the fuel debris sample due to the reaction to high temperatures during the accident and when the fuel debris migrated were identified and are useful for hypothesizing the fuel debris creation process.

Seawater

- Elements: Cl, Na, Mg, S, K, Ca, etc. ¹⁾

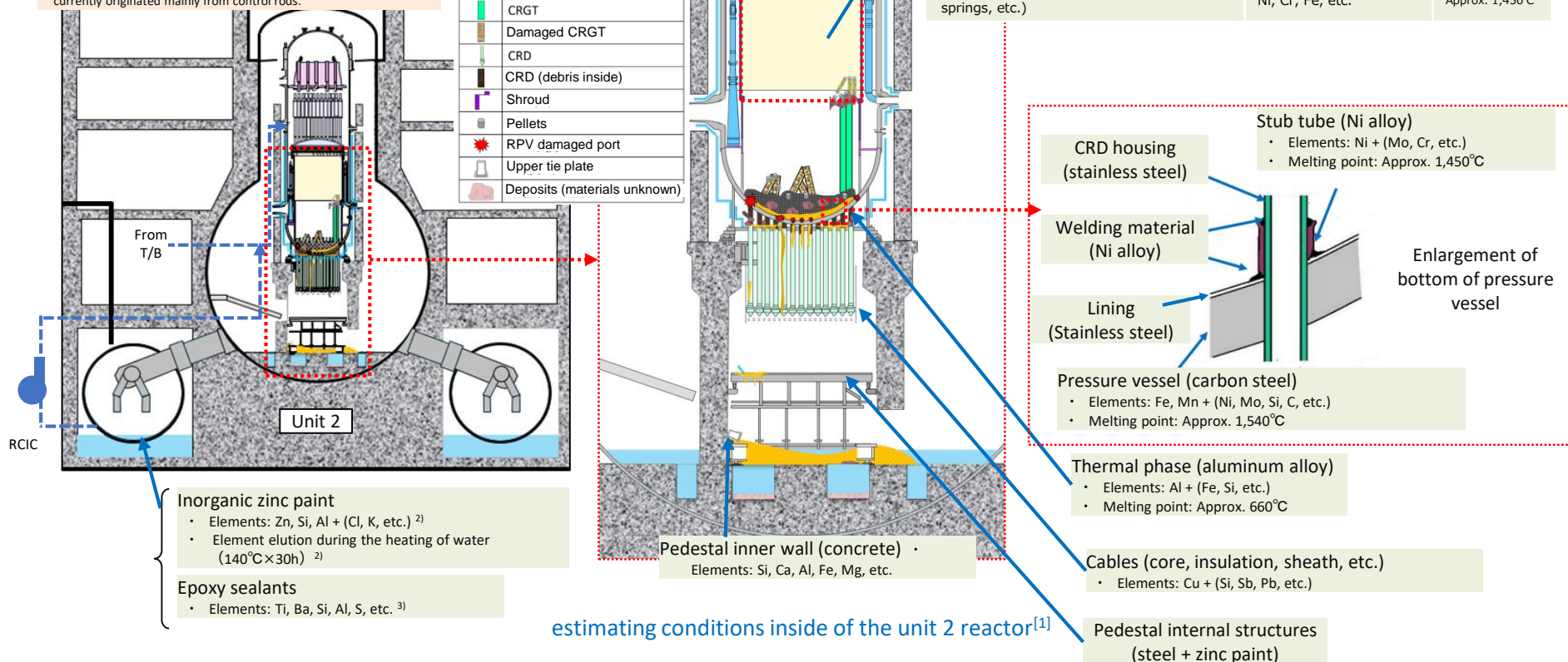
Boric acid ※ (Sodium pentaborate, boric acid)

※ Injected in 2012. Since boron was not detected in stagnant water in the PCV after injection ($B < 5 \text{ mg/L}^{(4)}$), it is assumed that the boron that exists currently originated mainly from control rods.



Light green: Materials that were originally present in the RPV and PCV
Light orange: Materials introduced following the earthquake

Major core materials	Major elements	Singular melting point
Uranium fuel	U, Gd, Pu, FP, MA	Approx. 2,800°C
Cladding tubes/CB (Zirconium alloy)	Zr, Sn, etc.	Approx. 1,760°C
Control rods, tie plates, and structures such as core support plates, etc. (stainless steel)	Fe, Cr, Ni, Si, Mo, etc.	Approx. 1,450°C
Neutron absorbance (boron carbide)	B, C	Approx. 2,450°C
Other fuel assembly parts (Ni alloy: spacer springs, etc.)	Ni, Cr, Fe, etc.	Approx. 1,450°C



¹⁾ Kirishima et al., J. Nucl. Sci. Technol. 52, (2015), 1240. ²⁾ Nakamori, et al., Atomic Energy Society of Japan 2018 spring conference, 2M17.

³⁾ TEPCO HD, Deliberations of TEPCO Fukushima Daiichi Nuclear Power Station Accident Analysis (28th meeting) Document 4-1. February 28, 2022 (SEM-EDX results)

⁴⁾ IRID, JAEA, (39th) Secretariat of the Team for Countermeasures for Decommissioning, Contaminated Water and Treated Water Treatment, metrial3-4-4, February 23, 2017. (Analysis results of stagnant water in the PCV)

[1] JAEA, Decommissioning/contaminated water/treated water countermeasure project beginning in 2023 (development of analysis/estimating technologies for ascertaining the attributes of still debris) 3. The development of technologies for estimating RPV damage and the behavior of migrating fuel debris inside the PCV-Final report.

– Example of past assessment of deposit/adhesion samples –

◆ TEM analysis results were used to identify the crystalline structure of phases that contain uranium, etc., and the creation conditions of those crystalline structures were used to estimate conditions inside the reactor during the accident. Since TEM analysis of the first fuel debris sample is ongoing, the following shows an example of an assessment based upon the analysis results from particles containing uranium in deposit/adhesion samples acquired during past internal investigations, etc.

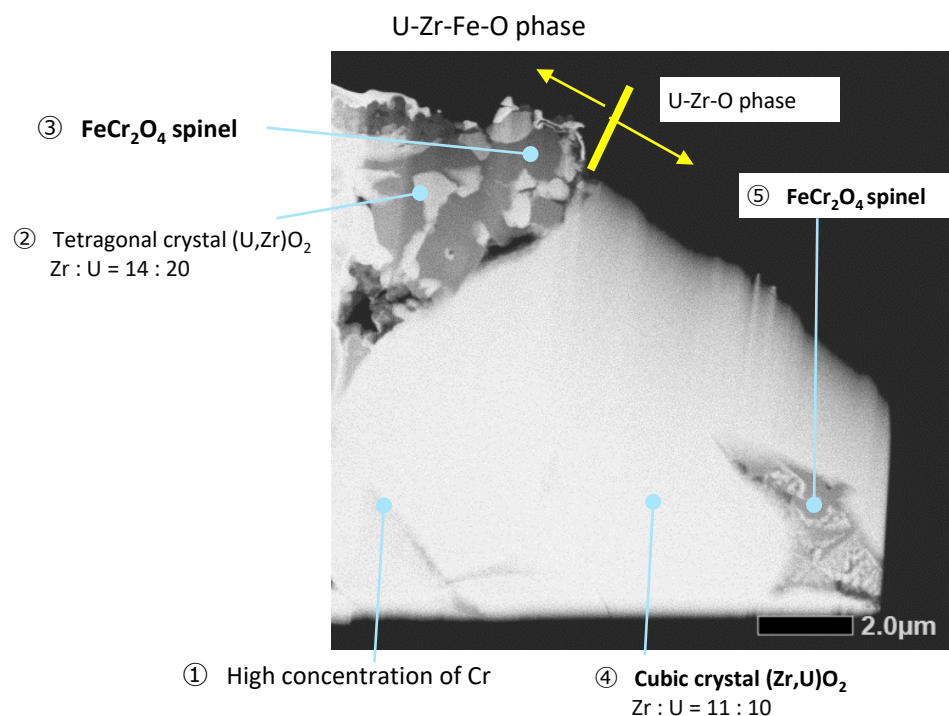


Figure 1 Analysis results sampled from the Unit 2 PCV penetration X-53 (TEM observation image from U particle cross-section)

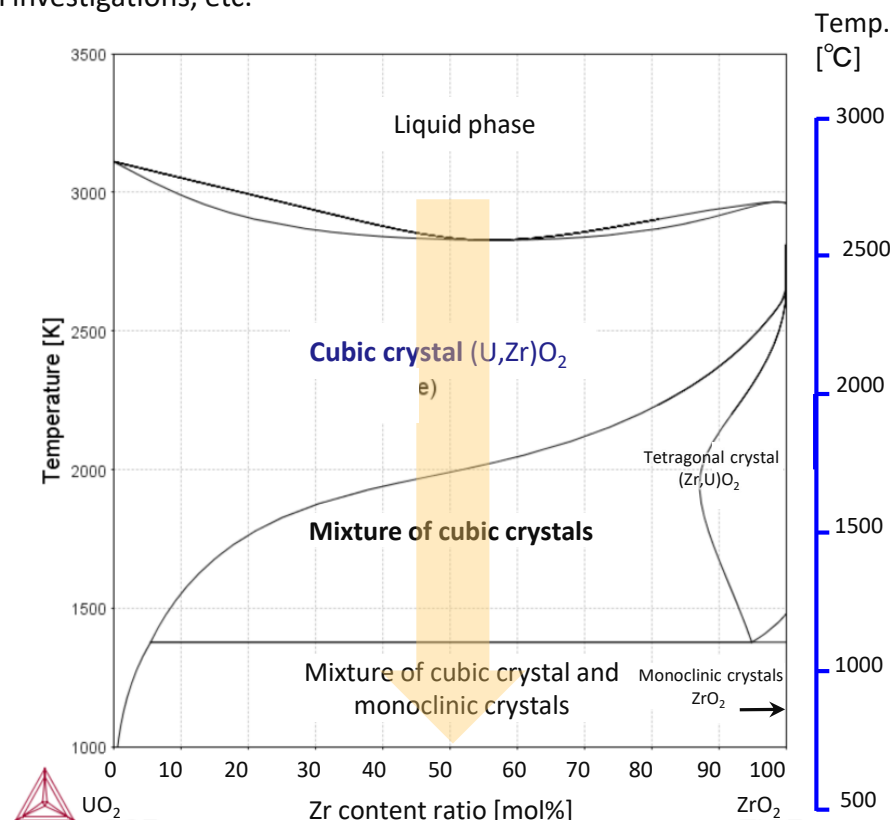


Figure 2 $\text{UO}_2\text{-ZrO}_2$ pseudo-binary system diagram ^[1]

[1] JAEA. Nuclear fuel/nuclear material thermodynamics database.

- When U particles contained in Unit 2 deposit/adhesion samples were analyzed using TEM, a cubic crystal $(\text{U,Zr})\text{O}_2$ with a U:Zr ratio of approx. 1:1 was observed. (Figure 1)
- As shown in Figure 2, for a single phase cubic crystal $(\text{U,Zr})\text{O}_2$ to form, it is estimated that temperature must exceed approx. $2,000^\circ\text{C}$ and then quickly cool before any other phases can form after the cubic crystal $(\text{U,Zr})\text{O}_2$ has formed.

Analysis method abbreviation	Analysis method name	Analysis method overview
ICP-AES	Inductively coupled plasma atomic emission spectroscopy	Qualitative and quantitative analysis method of elements by introducing atomized samples into high-temperature plasma and obtaining element-specific spectra by spectroscopy of the issued light.
ICP-MS	Inductively coupled plasma mass spectrometry	Method of measuring the concentration of elements and its isotopes by introducing atomized samples into high-temperature plasma, ionizing elements in the sample and measuring the number of ions in ion mass-to-charge ratio (m/z) by mass spectrometry.
TIMS	Thermal ionization mass spectrometry	Method of measuring the concentration of elements and its isotopes by applying samples onto metal filament, ionizing the atoms by heating under vacuum and measuring the number of ions in ion mass-to-charge ratio (m/z) by mass spectrometry.
IDMS	Isotope dilution mass spectrometry	Method for measuring the elemental mass (concentration) of a specimen targeted for analysis (analyte) by adding a known amount of a rare isotope with a totally different isotopic composition and measuring changes to the isotopic composition mass of the analyte before and after the changes and the amount of standard sample added. Isotopic composition is measured through mass spectrometry.
SEM	Scanning electron microscope	Device that can observe the sample surface by irradiating the surface with electron beams, and can also analyze elements by attaching an X-ray analyzer.
EDX	Energy dispersive X-ray spectroscopy	Method of elemental analysis and compositional analysis by detecting characteristic X-rays generated by electron irradiation and categorizing them by the energy of characteristic X-rays.
WDX	Wavelength dispersive X-ray spectroscopy	Method of elemental analysis and compositional analysis by detecting characteristic X-rays generated by electron irradiation and performing spectroscopy at the wavelength of characteristic X-rays.
TEM	Transmission electron microscope	Method of imaging electrons transmitted through the sample and scattered electrons for observation under high magnification by irradiating thinned samples with electron beams, and also conducting elemental analysis by attaching an X-ray analyzer. Crystal structure can also be obtained from the diffraction image.
SIMS	Secondary ion mass spectrometry	Method of measuring the concentration of elements and its isotopes by measuring the secondary ions generated by irradiating the sample surface with a beam of ions with a mass spectrometer and measuring the number of ions in ion mass-to-charge ratio (m/z) by mass spectrometry.
Raman spectroscopy	Micro Raman spectroscopy	Method of obtaining properties such as molecular structure, temperature, stress, electrical properties, orientation and crystallinity by irradiating the sample surface with light and dispersing Raman scattering light. Information on chemical form of micro-regions on μm order can be obtained by combining Raman spectroscopy with conventional optical microscopes.

Analysis method abbreviation	Analysis method name	Analysis method overview
X-ray CT	X-ray computed tomography	Method of obtaining density distribution of the sample interior by irradiating the sample with X-rays, capturing the transmitted X-ray intensity by a computer and scanning it three-dimensionally. Distribution of phases of different density can be obtained.
XAFS	X-ray absorption fine structure spectroscopy	Method of analyzing the internal structure of materials at the molecular and atomic level by irradiating the sample with X-rays and precisely observing the absorbed X-ray energy
XRF	X-ray fluorescence spectroscopy	Method of qualitative analysis of content of constituent elements by measuring the wavelength and energy of X-rays (X-ray fluorescence) generated according to the substance by irradiating the sample with X-rays
XRD	X-ray diffraction analysis	Method of analyzing the crystal structure, crystal orientation, crystal lattice size, etc. of the object by irradiating the sample with X-rays and measuring the resulting X-rays (diffracted X-ray)
IP	Imaging plate	Radiation image measuring instrument that detects radiation energy as stimuable luminescence. Dose distribution of the sample can be obtained.

The following 3 types of analysis are used to analyze the fuel debris sample and identify its characteristics and how it was formed.

● Non-destructive analysis

[Overview] Roughly grasp information, such as distribution of pores and high-density materials and contained components, without changing the state of the received sample as much as possible.

[Purpose] Obtain basic information of the sample, and confirm the presence or absence of components derived from nuclear fuel (uranium, radioactive nuclides, etc.) early on. Additionally, review how to specifically proceed with the analysis, such as which area to focus on in the solid analysis and liquid analysis to be conducted later on and which data to be obtained in what precision.

[Analysis methods] External appearance, weight, dose rate, IP, X-ray CT, γ -ray spectrometry, SEM-WDX (surface)

● Solid analysis

[Overview] Confirm what kind of state uranium, zirconium and other components from the reactor are in (what the coexisting elements are, whether it retains its pre-accident state, whether it is oxidized, etc.), by fractionating parts of the sample and observing its cross section in detail.

[Purpose] Obtain information on “how the sample was formed”, such as which materials reacted under what temperature or atmosphere* to form the sample.

*The synchrotron analysis of SPring-8, which was newly added after the previous report, is considered to enable more accurate estimation of the temperature and atmosphere at the time of the accident, since more detailed data than the conventional observation method based on electron microscopes can be obtained such as three-dimensional distribution of elements in the sample and valence of uranium.

[Analysis methods] SEM-EDX, SEM-WDX, TEM-EDX, SIMS, Raman spectroscopy, μ -XAFS, μ -XRF, μ -XRD

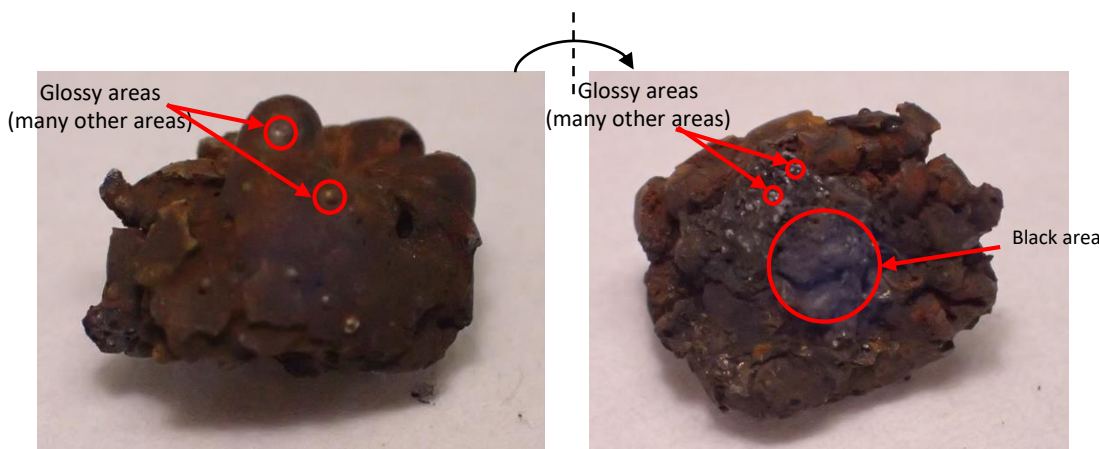
● Liquid analysis

[Overview] Fractionate part of the sample and dissolve it in acid to measure the elements and nuclide content in the resulting dissolving solution.

[Purpose] Obtain necessary information to review the process to safely retrieve and stably store fuel debris, such as uranium isotope ratio and radioactive nuclide concentration.

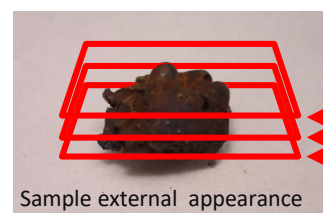
[Analysis methods] ICP-MS, ICP-AES, TIMS, γ -ray spectrometry, α -ray spectrometry

Continuing the series of analyses will gradually identify the characteristics of fuel debris deposited in the core and contribute to safety evaluation and rationalization for fuel debris retrieval and storage.



Size: Approx. 9mm × Approx. 7mm (compared with a scale)

Figure 1 External appearance of fuel debris sample (after arrival at JAEA Oarai)



【Measurement method】

- Images taken vertically at 0.2 mm intervals after putting the sample into a polypropylene canister. A total of 38 images were obtained.
- CT values (showing the correlation to density) were color-coded in order to ascertain areas of high density and low density.

Cross-section A
Cross-section B
Cross-section C

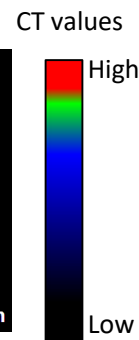
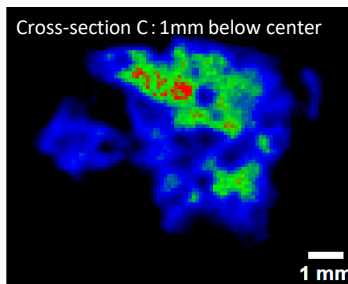
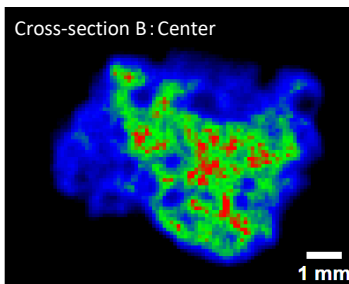
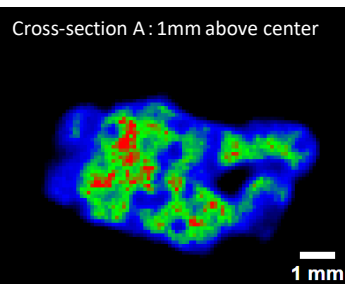


Figure 2 Fuel debris sample x-ray CT images

○ External appearance, mass, dose rate

- The received sample was reddish-brown overall with an indefinite shape. Black and glossy areas could be seen on the surface. (Figure 1)
- Mass: 0.693g
- Dose rate: Approx. 8mSv/h (γ-rays) ※1

※1 An ionization chamber was used to measure the sample while it was still inside a polypropylene container (at a distance of 1~2 cm from the sample))
IP imagery (dose distribution) could not show an accurate distribution due to the high dose rates and small size of the sample.

○ X-ray CT

- Relatively high-density areas (red) and pores (black) profound inside the sample. (Figure 2)
- Results calculated from the x-ray CT image found the volume ※2 to be approx. 0.1cm³.
→ Density estimated to be approx. 7g/cm³ from the aforementioned mass and volume.

※2 Includes internal pores but excludes surface pores

- Since Am-241, which is produced by neutron capture reaction of U-238 in the nuclear fuel, is detected in addition to Eu-154, the sample is considered to contain nuclear fuel components.

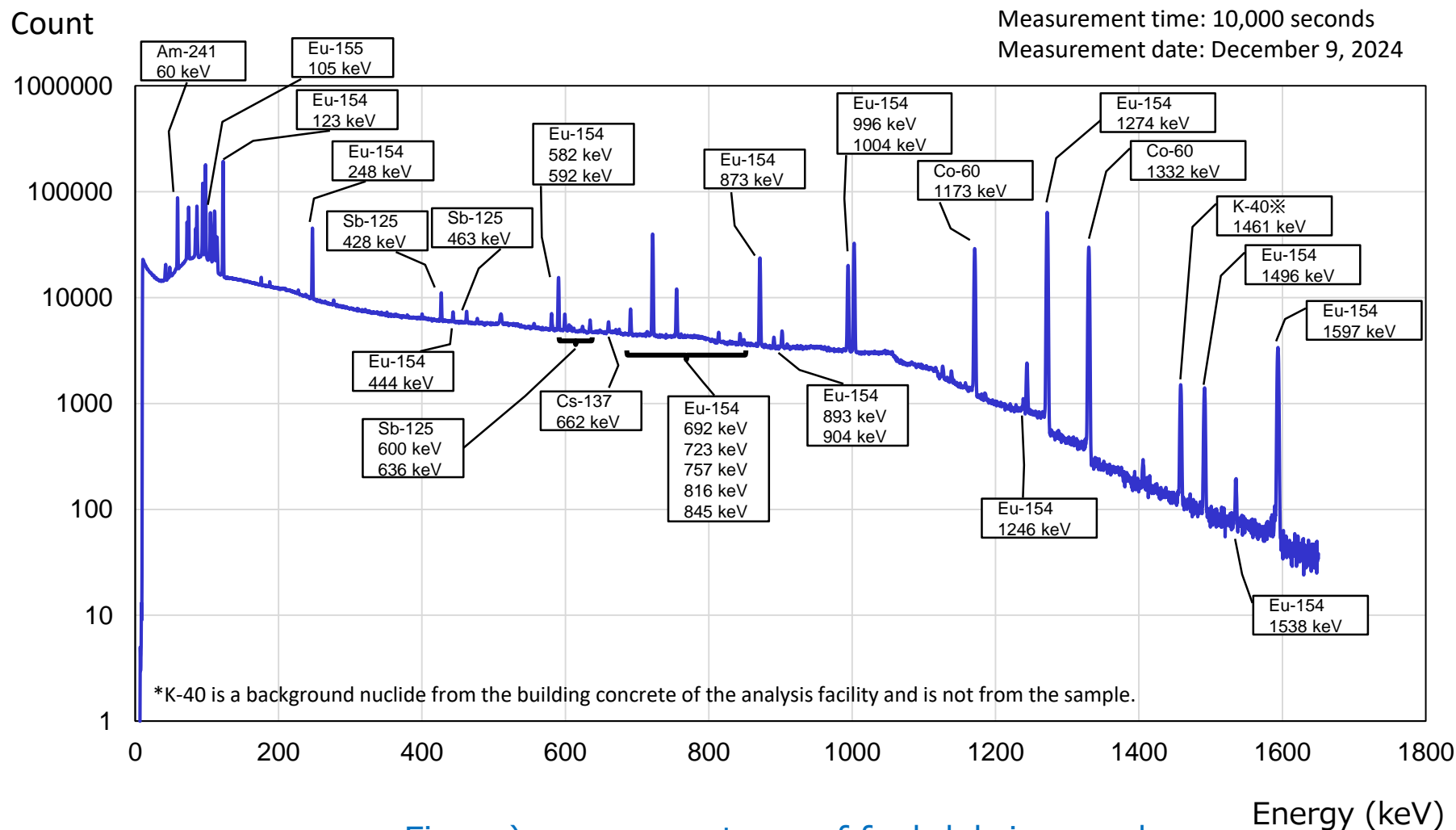
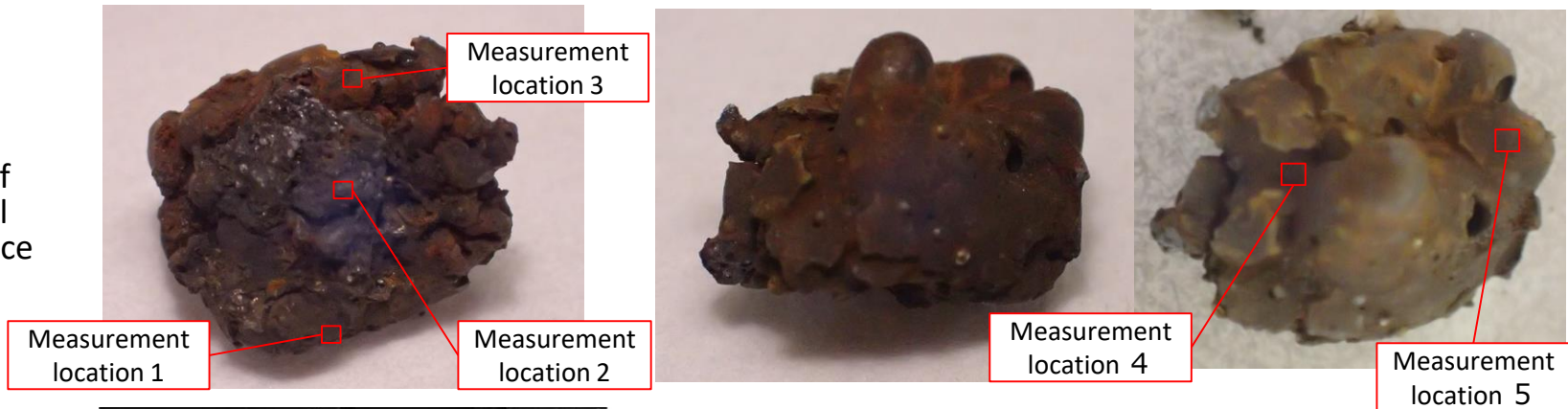


Figure) γ -ray spectrum of fuel debris sample

- In order to review the policy for detailed analysis of the sample, element distribution of the sample surface was determined with SEM-WDX area analysis.
 - 5 measurement locations were selected away from each other on the front and back sides of the sample, in order to obtain extensive information of the sample surface (see measurement locations 1-5 below; measurement location 1 is the same as the previous report).
 - Area analysis was conducted after point analysis.
 - In addition to U, Fe (common to all measurement locations), major elements that were identified with the point analysis spectrum were added as elements to be measured in area analysis (the number of elements to be measured per field of view is limited to 4-5 elements in order to secure the analysis period).

Photo of
external
appearance



SEM observation
results

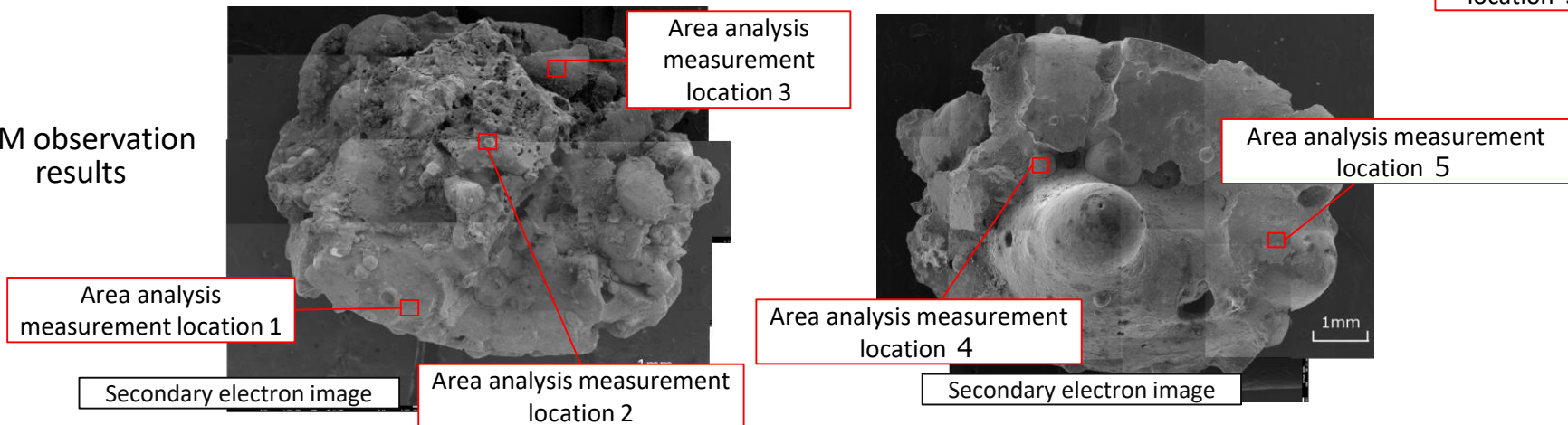


Figure1 Measurement locations of SEM-WDX area analysis of the fuel debris sample surface

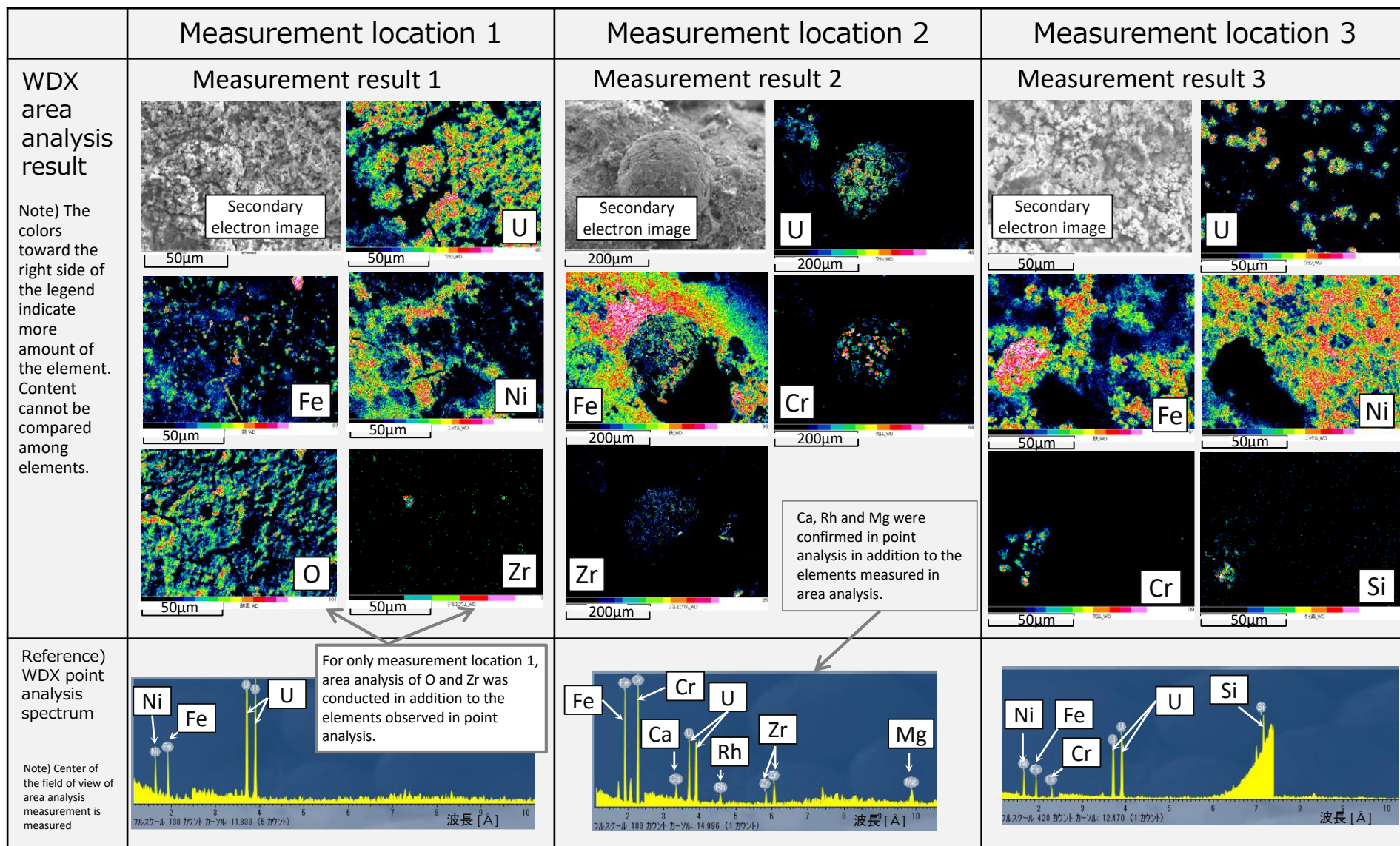
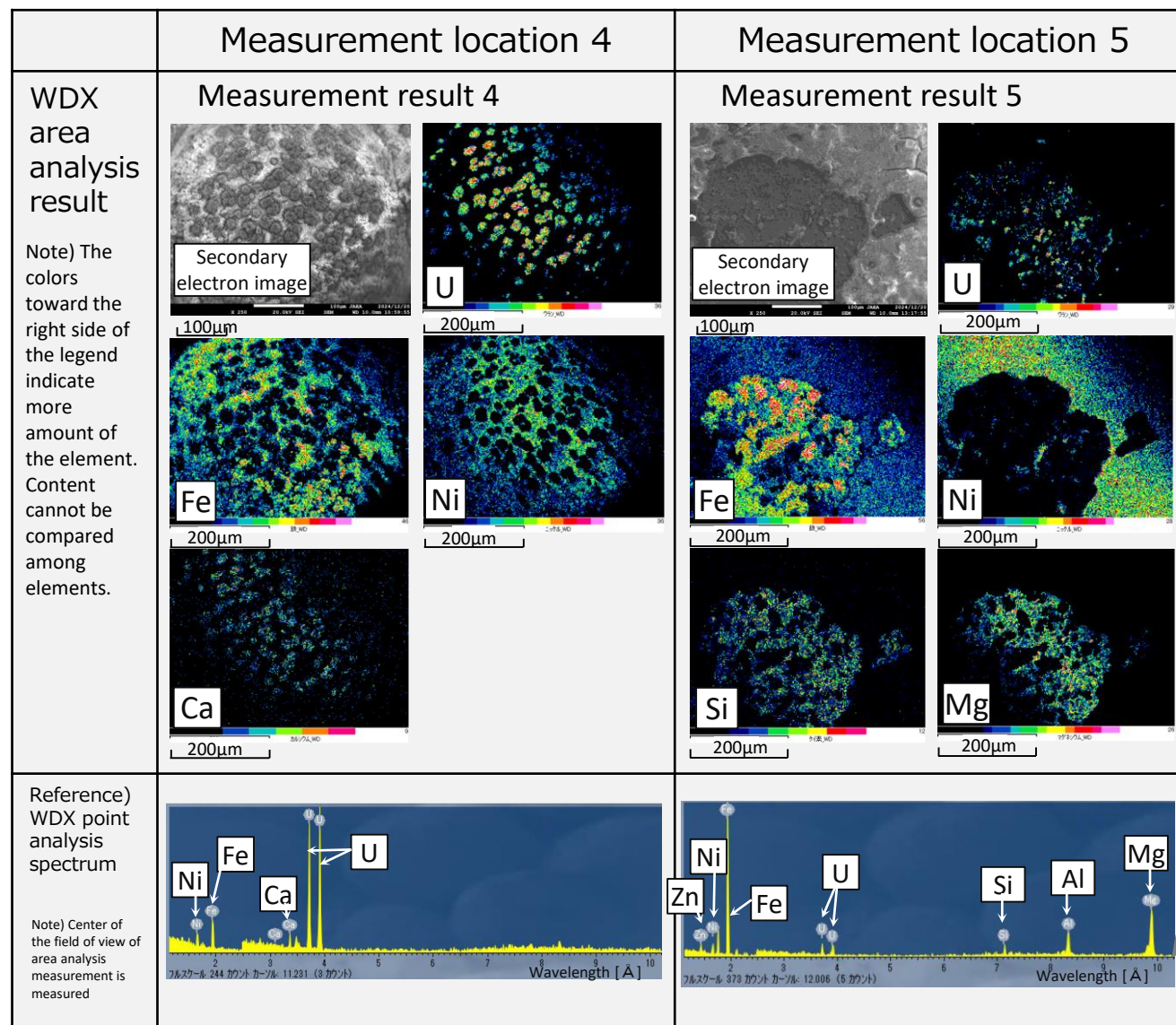


Figure2 SEM-WDX measurement results of fuel debris samples(Measurement location 1-3)



- U and Fe were observed on all fields of view. However, the location of U does not match with the location of Fe. Some fields of view also suggested less U and more Fe (Measurement location 5).

⇒ The fuel debris sample is heterogeneous, but U is considered to be widely distributed at least on the sample surface.

Figure3 SEM-WDX measurement results of fuel debris samples
(Measurement location 4-5)

Zn and Al were confirmed in point analysis in addition to the elements measured in area analysis.

Outer diameter
of specimen
container:
Approx. 1.8cm



Block[A-1] :

JAEA Oarai



Approx. 7mm

Block[D] :

NDC



Block[C] :

NFD



Particles[B] :

JAEA NSRI



Particles[A-2] :

JAEA Oarai+SPring-8



Approx. 3mm



Focused elements/nuclides during liquid analysis

Items	Units	Focused elements/nuclides	Analysis methods
Element content ratio	mg/100mg specimen (Mass of each element per hundred milligrams of the sample)	<ul style="list-style-type: none"> • U (Fuel) , Zr (Cladding tubes/CB) • Fe, Cr, Ni (Carbon steel, stainless steel, etc.) • Si, Ca, Al, Mg (Instrument materials, seawater, concrete, etc.) • B (^{10}B), Gd (^{155}Gd, ^{157}Gd) (Neutron poison) • Pb, Zn, Ti (Shielding material, paint, etc.) • Mo, Sb (Grease, instrumentation, FP, etc.) • Other elements found through qualitative analysis or SEM 	<ul style="list-style-type: none"> • ICP-AES • ICP-MS • IDMS
Isotope ratio	Molar ratio [-]	<ul style="list-style-type: none"> • U Isotope : $^{235}\text{U}/^{238}\text{U}$ ratio or $^{235}\text{U}/\text{U}_{\text{total}}$ ratio $\text{U}_{\text{total}} = ^{234}\text{U} + ^{235}\text{U} + ^{236}\text{U} + ^{238}\text{U}$ 	<ul style="list-style-type: none"> • TIMS • ICP-MS
		<ul style="list-style-type: none"> • Pu Isotope • Nd Isotope (Conversion rate indicator) • Gd Isotope 	<ul style="list-style-type: none"> • TIMS (Element mass assessed with IDMS)
Radioactivity concentration	MBq/g (Radioactivity for each nuclide per sample mass)	<ul style="list-style-type: none"> • γ-ray emitting nuclides • α-ray emitting nuclides • ^{90}Sr 	<ul style="list-style-type: none"> • γ-ray spectrometry • α-ray spectrometry • ICP-MS/MS

◆ NDC solution analysis

○ Element content ratio → Chart 1

- Block[D] was further crushed and approx. 0.1g of the particles obtained was pressure melted in heated acid.
- ICP-AES and ICP-MS were used to measure the quantity of elements in the obtained liquid.
- Approx. 5% of the specimen mass was undissolved residue (primarily Fe-Cr oxide), so element content was assessed using SEM-EDX to estimate the element content of the undissolved residue.
- The ratio of elements contained in the sample were assessed by combining the analysis values for the element content of the liquid with the estimates of the element content of the undissolved residue.

○ Isotope ratio (U) → Chart 2

- The amounts of ^{234}U , ^{235}U , ^{236}U and ^{238}U in the liquid was measured using ICP-MS.

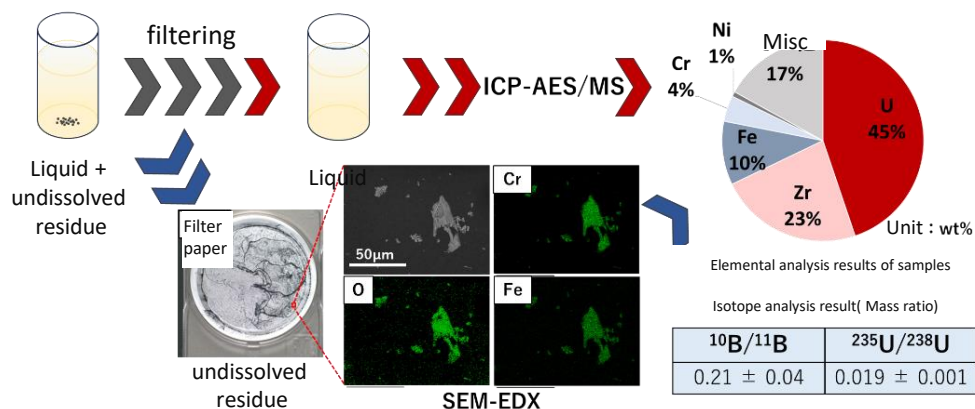


Figure 1 NDC element content ratio assessment flow

Chart 1 Element content ratio assessment results

k=2 Expanded uncertainty

Element	Element content ratio [mg/100mg specimen]
U	45 ± 2
Zr	23 ± 1
Fe	10.2 ± 0.8
Cr	4 ± 1
Ni	0.79 ± 0.03
Si	<0.9
Ca	0.22 ± 0.02
Al	<0.3
Mg	0.098 ± 0.005
B	0.049 ± 0.004
Gd	0.39 ± 0.05
Mo	0.123 ± 0.007
Sb	<0.003
Pb	<0.006
Zn	0.062 ± 0.003
Ti	<0.03
Mn	0.42 ± 0.02
Na	0.087 ± 0.006
Nb	0.090 ± 0.008
Sn	0.033 ± 0.001

Chart 2 Uranium isotope ratio analysis results

k=2 Expanded uncertainty

Nuclide	U isotope ratio ^{※1} [at%]
$^{234}\text{U}/\text{U}$	0.026 ± 0.002
$^{235}\text{U}/\text{U}$	1.9 ± 0.1
$^{236}\text{U}/\text{U}$	0.33 ± 0.02
$^{238}\text{U}/\text{U}$	97.7 ± 0.2

※1 Ratio of U = $^{234}\text{U} + ^{235}\text{U} + ^{236}\text{U} + ^{238}\text{U}$

◆ JAEA NSRI liquid analysis

○ Element content ratio → Chart 1

- Approx. 0.1g of **particles[B]** was dissolved in an alumina crucible with alkaline flux※, and the resulting molten material was dissolved in hot nitric acid.
 ※ Alkali melting: By taking fuel debris, which is difficult to dissolve in acid, and heating/dissolving it in alkaline flux (sodium peroxide) to convert it to a substance that is easily dissolved in acid, we can obtain a uniform solution without undissolved residue.
- The amount of the elements contained in the obtained solution was measured using ICP-AES to assess the element content ratio of the sample.
- U, Pu, Nd and Gd were separated from the solution using UTEVA[®] resin and anion exchange resin after which IDMS was used to measure the amount of the elements in the separated solutions.

○ Isotope ratio (U, Pu, Gd and Nd) → Chart 2

- The separated solutions of each element obtained in “Element content ratio” above were then measured using TIMS.

○ Radioactivity concentration → Chart 3

- For γ-ray emitting nuclides, a small amount was fractionated from the obtained solution to measure radioactivity with γ-ray spectrometry.
- For ²⁴¹Am and ²⁴⁴Cm, TRU resin was used to separate Am and Cm from the obtained solution and α-ray spectrometry was used to measure the radioactivity of the separated solution.
- For ⁹⁰Sr, Sr resin was used to separate Sr from the obtained solution and ICP-MS/MS was used to measure the amount of ⁹⁰Sr isotopes in the obtained solution.

Chart 1 Element content ratio assessment results

k=2 Expanded uncertainty

Element	Element content ratio [mg/100mg Specimen]	Notes
U	29.9 ± 0.2	IDMS measurement
Zr	19 ± 2	
Fe	16 ± 1	
Cr	4.8 ± 0.2	
Ni	2.6 ± 0.1	
Si※ ¹	0.05 ± 0.01※ ¹	Reference value ※ ¹
Ca	0.29 ± 0.02	Revised value for the amount of Ca in the flux
Al		Excluded since it originates from the crucible
Mg※ ¹	0.16 ± 0.01※ ¹	Reference value ※ ¹
B※ ¹	0.05 ± 0.01※ ¹	Reference value ※ ¹
Gd	0.239 ± 0.002	IDMS measurement
Mo	0.21 ± 0.01	
Sb		Undetected by ICP-AES qualitative analysis
Pb		Undetected by ICP-AES qualitative analysis
Zn	0.08 ± 0.01	
Ti	0.02 ± 0.01	
Mn	0.43 ± 0.02	
Na		Excluded since it originates from the flux
Nb		Undetected by ICP-AES qualitative analysis
Sn	0.13 ± 0.01	
Pu	0.084 ± 0.001	IDMS measurement
Nd	0.098 ± 0.001	IDMS measurement

※¹ In regards to the element concentration in the solution the concentration ratio of operational gaps to solution is 0.1 or higher, reference value.

◆ JAEA NSRI solution analysis (cont.)

Chart 2 TIMS isotope ratio analysis results

k=2 Expanded uncertainty		
Element	Nuclide	Isotope ratio※1 [at%]
U	²³⁴ U	0.027 ± 0.001
	²³⁵ U	1.943 ± 0.002
	²³⁶ U	0.342 ± 0.001
	²³⁸ U	97.689 ± 0.001
Pu	²³⁸ Pu	1.446 ± 0.001
	²³⁹ Pu	64.857 ± 0.001
	²⁴⁰ Pu	23.915 ± 0.001
	²⁴¹ Pu	5.450 ± 0.001
	²⁴² Pu	4.332 ± 0.001
Nd	¹⁴² Nd	8.79 ± 0.01
	¹⁴³ Nd	17.85 ± 0.01
	¹⁴⁴ Nd	29.46 ± 0.02
	¹⁴⁵ Nd	14.27 ± 0.01
	¹⁴⁶ Nd	16.90 ± 0.01
	¹⁴⁸ Nd	8.00 ± 0.02
	¹⁵⁰ Nd	4.72 ± 0.04
Gd	¹⁵² Gd	0.12 ± 0.01
	¹⁵⁴ Gd	2.05 ± 0.01
	¹⁵⁵ Gd	3.85 ± 0.01
	¹⁵⁶ Gd	31.37 ± 0.01
	¹⁵⁷ Gd	3.19 ± 0.01
	¹⁵⁸ Gd	37.71 ± 0.01
	¹⁶⁰ Gd	21.71 ± 0.01

※1 Ratio of all isotopes for each element (nuclides noted in the chart)

Chart 3 Radioactivity concentration assessment results

k=2 Expanded uncertainty	
Nuclide	Radioactivity concentration※1 [MBq/g-specimen]
⁶⁰ Co	2.6 ± 0.3
¹²⁵ Sb	1.0 ± 0.2
¹³⁴ Cs	<0.030
¹³⁷ Cs	0.21 ± 0.04
¹⁵⁴ Eu	13 ± 2
¹⁵⁵ Eu	4.0 ± 0.5
²⁴¹ Am	19 ± 2
²⁴³ Am	<1.8
²⁴⁴ Cm	8.3 ± 1.0
⁹⁰ Sr	(1.9 ± 0.2) × 10 ²

※1 Values as of the date of measurement

The analysis methods for each nuclide and the dates of measurement are as follows:

- For ⁶⁰Co, ¹²⁵Sb, ¹³⁴Cs, ¹³⁷Cs, ¹⁵⁴Eu and ¹⁵⁵Eu, small samples were fractionated from the obtained solution and radioactivity was measured using γ-ray spectrometry. (Measurement date: April 17, 2025)
- For ²⁴¹Am, ²⁴³Am and ²⁴⁴Cm, Am and Cm were separated from the solution using column separation and the obtained separated solutions were subjected to α-ray spectrometry to measure the radioactivity of each nuclide. (Measurement date: May 22, 2025)
Furthermore, for ²⁴⁴Cm, since peak ²⁴³Cm cannot be separated and the radioactivity of ²⁴⁴Cm is sufficiently great, only ²⁴⁴Cm was assessed.
- For ⁹⁰Sr, Sr resin was used to separate Sr from the obtained solution and the weight of ⁹⁰Sr isotopes was measured using ICP-MS/MS. (Measurement date: June 17, 2025)

◆ JAEA Oarai liquid analysis

○ Element content ratio → Chart 1

- Approx. 0.01g was sampled from [particles\[A-2\]](#) and dissolved in hot nitric acid (with a small amount of hydrofluoric acid added).
- The quantity of targeted nuclides in the obtained solution was measured with ICP-MS, and the nuclide content was converted to element content while referring to fuel composition and the composition of naturally occurring isotopes.
- Approx. 7% of the specimen mass was undissolved residue (primarily Fe-Cr oxide), so element content was assessed using SEM-EDX to estimate the amount of elements contained in the undissolved residue.
- The element content ratio in the sample were assessed by combining the analysis values for the element content of the solution with the estimates of the element content of the undissolved residue.

○ Isotope ratio (U) → Chart 2

- The amount of ^{234}U , ^{235}U , ^{236}U and ^{238}U in the solution was measured with ICP-MS.

Chart 2 Uranium isotope ratio analysis results

Nuclide	Isotope ratio ^{※1} [at%]
$^{234}\text{U}/\text{U}$	0.027 ± 0.002
$^{235}\text{U}/\text{U}$	1.93 ± 0.01
$^{236}\text{U}/\text{U}$	0.35 ± 0.01
$^{238}\text{U}/\text{U}$	97.7 ± 0.7

※1 Ratio of U = $^{234}\text{U} + ^{235}\text{U} + ^{236}\text{U} + ^{238}\text{U}$



[Particles\[A-2\]](#) obtained through crushing



Sample specimen
(Approx. 0.01g)

Sample used for liquid analysis

Chart 1 Element content ratio analysis results

k=2 Expanded uncertainty

Element	Element content ratio mg/100mg
U	25.5 ± 0.8
Zr	16 ± 3
Fe	20 ± 2
Cr	3 ± 1
Ni	9.9 ± 0.3
Si	<LOQ
Ca	<LOQ
Al	<LOQ
Mg	<LOQ
B	<LOQ
Gd	0.192 ± 0.009
Mo	0.349 ± 0.009
Sb	<LOQ
Pb	<LOQ
Zn	<LOQ
Ti	0.05 ± 0.01

◆ JAEA Oarai liquid analysis (cont.)

○ Radioactivity concentration

- γ-ray spectrometry
 - ^{60}Co , ^{125}Sb , ^{137}Cs , ^{154}Eu and ^{241}Am were detected. (Figure 1 top. Same nuclides that were detected during non-destructive analysis)
 - The same nuclides were detected in the undissolved residue, but the intensity of ^{60}Co was relatively high. (Figure 1, bottom)
- α-ray spectrometry
 - ^{242}Cm , $^{243}\text{Cm}+^{244}\text{Cm}$, $^{241}\text{Am}+^{238}\text{Pu}$ and $^{239}\text{Pu}+^{240}\text{Pu}$ were detected in the solution

Chart 3 Radioactivity concentration assessment results

k=2 Expanded uncertainty

Nuclide	Radioactivity concentration ^{※1} [MBq/g-specimen]
^{60}Co	2.0 ± 0.5
^{125}Sb	2.0 ± 0.5
^{137}Cs	0.6 ± 0.2
^{154}Eu	1.8 ± 0.5
^{241}Am	2.3 ± 0.6
^{242}Cm	0.02 ± 0.02
$^{243}\text{Cm}+^{244}\text{Cm}$	3.5 ± 0.2
$^{241}\text{Am}+^{238}\text{Pu}$	11.5 ± 0.4
$^{239}\text{Pu}+^{240}\text{Pu}$	4.8 ± 0.3

※1 Values as of the date of measurement

•For ^{60}Co , ^{125}Sb , ^{137}Cs , ^{154}Eu and ^{241}Am , small samples were fractionated from the obtained solution and radioactivity was measured using γ-ray spectrometry. (Measurement date: April 17, 2025)

•For ^{242}Cm , $^{243}\text{Cm}+^{244}\text{Cm}$, $^{241}\text{Am}+^{238}\text{Pu}$ and $^{239}\text{Pu}+^{240}\text{Pu}$, small amounts were taken from the obtained solution and smeared on a SUS plate after which α-ray spectrometry was used to measure the radioactivity of each nuclide. (Measurement date: May 13, 2025)

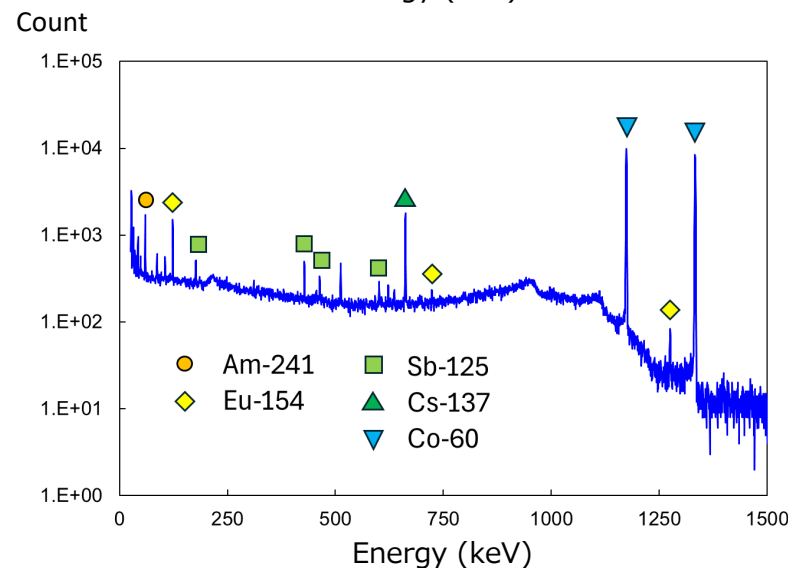
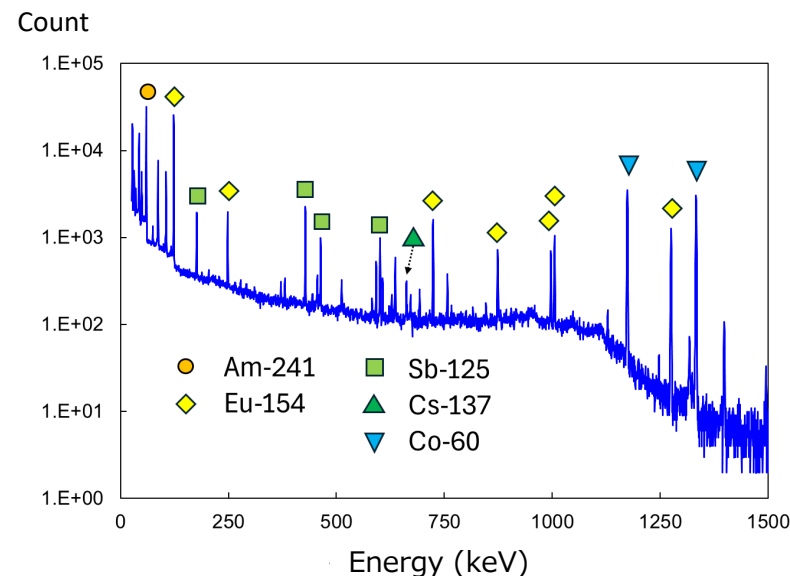


Figure γ-ray spectrometry Top: Solution, Bottom: Undissolved residue

Top: Measurement date: March 17, 2025, measurement time: 5,000 seconds,
bottom: measurement date: March 18, 2025, measurement time: 10,000 seconds

Material Adhesions to X-6 penetration investigation device



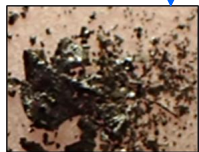
(Obtained in 2020)
Smear samples taken from the surface of the end of the investigation device. A portion of the smear paper was cut into batches and subjected to liquid analysis.

Fuel debris sample



(Obtained in FY2024)
Sampled during first trial retrieval. Crushed, fractionated and subjected to liquid analysis.

Obtained sample



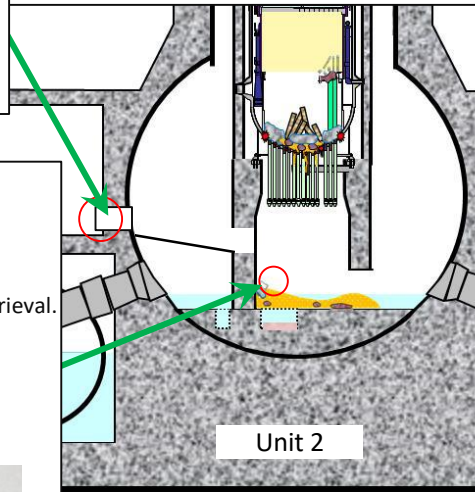
Particles [B]



Block [D]



Particles [A-2]



- It is presumed that the PCV penetration (X-6 penetration) contains substances originating from fuel that migrated from the pressure vessel to the pedestal during the accident. Uranium isotopic composition and element ratio were compared for reference when generating a hypothesis about the process by which the fuel debris sample was created.
- U isotopic composition: Same as the core mean (refer to page 8) and the X-6 penetration sample. (see the chart below)
- Zr/U ratio (atomic ratio): Percentage of Zr is higher than the core mean (approx. 1.3. Refer to page 7) and the X-6 penetration sample. (see the chart below)
- Gd/U ratio: Core mean is approx. 0.75wt% of U weight while the measurement results from the fuel sample show approx. around 0.80wt%. (No quantitative data for the X-6 penetration sample)

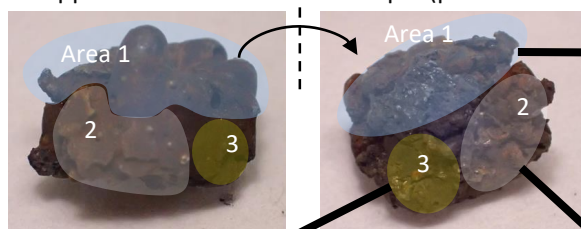
Liquid analysis results (example of comparison between fuel debris sample and X-6 penetration sample)

Sample	U isotopic composition [at%]			Zr/U ratio (Atomic ratio)	Gd/U ratio [wt%]	
	²³⁴ U/U	²³⁵ U/U	²³⁶ U/U			
Fuel debris sample						
Particles 【B】	0.027±0.001	1.943±0.002	0.342±0.001	1.7±0.2	0.80±0.01	
Block 【D】	0.026±0.002	1.9±0.1	0.33±0.002	1.33±0.08	0.9±0.1	
Particles 【A-2】	0.027±0.002	1.93±0.01	0.35±0.01	1.6±0.3	0.75±0.04	
Material adhered to X-6 penetration investigation device (Data source: [1])						
Material adhered -2	0.03±0.03	1.91±0.03	0.34±0.03	1.03±0.02	No data since results Gd was not measured	

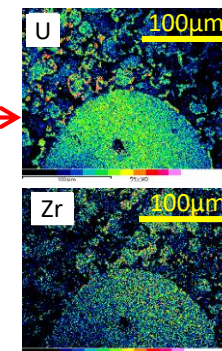
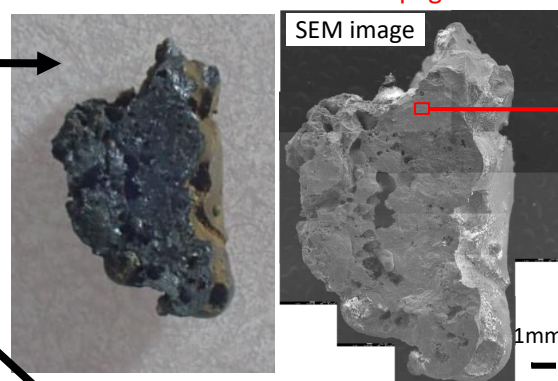
Expanded uncertainty expressed as k=2

- In order to deliberate analysis conditions and which elements to focus on during detail analysis (solid analysis and liquid analysis), and the distribution of elements on the fractured surface, each fractured piece of the sample (≡ inside the fuel debris sample) was examined.
- Since the comprising elements and microstructures of the cross-section, such as the generation of a coarse Zr-U-O phases (see photos below), were found to be almost the same throughout each of the fractured pieces, it was assumed that each fractured piece was generated through the same process and each of the different regions were subjected to solid analysis and liquid analysis.
- Overall, the fragments are made up of composite phases of U-Zr-Fe-Cr-Ni-O with localized areas of small amounts of Mg, Al, Si, Sn, etc., so in addition to the primary reactor core materials, a small number of other elements and the distribution of those elements were focused on. (Refer to the following pages for details)

External appearance of fuel debris sample (prior to crushing)

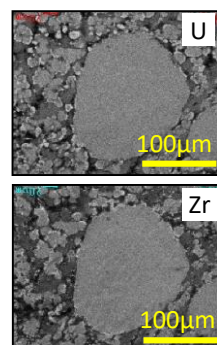
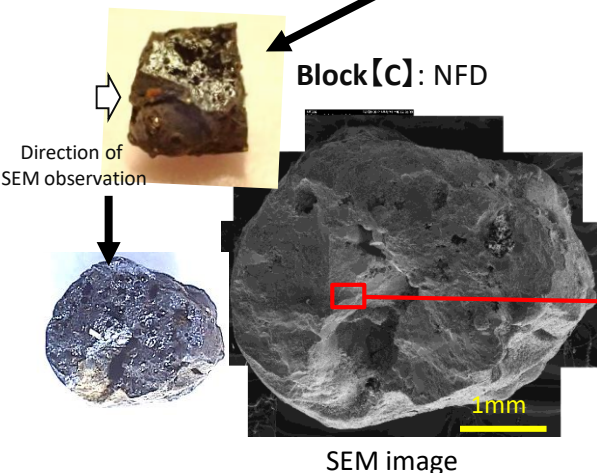


Block[A-1]: JAEA Oarai ⇒ page 36



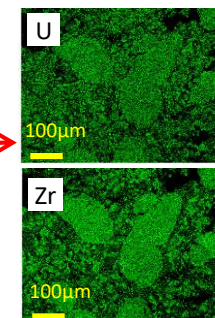
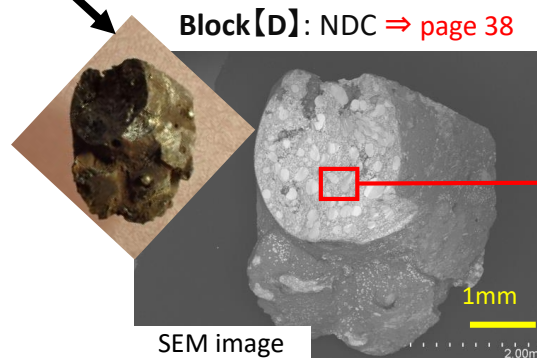
U and Zr element map
(More color as shown on the right side of the key indicates larger quantities)

Block[C]: NFD



U and Zr element map
(Whiter areas indicate greater quantities)

Block[D]: NDC ⇒ page 38



U and Zr element map
(Dark green indicates greater quantity)

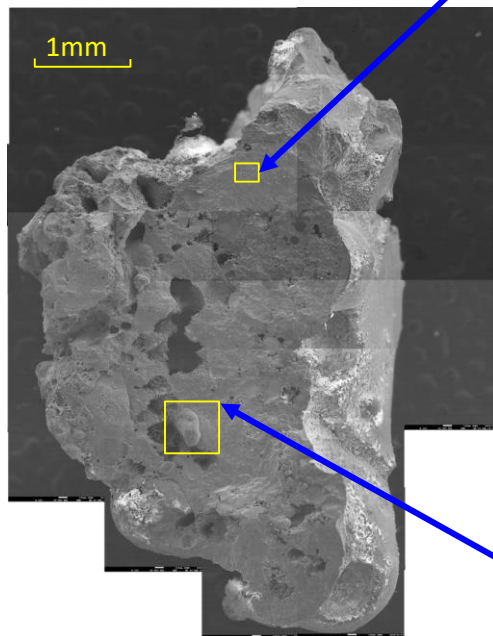
Cut and analyzed in detail ⇒ page 39

Zr-U-O phase* on the surface of each fragment

* Quantifying each element is difficult since the observed fractured surface is not smooth, but since there are approximately the same amounts of U and Zr, and the coarse Zr-U-O phase, and shape of that phase, observed in the cross-section (to be referred to later) resembles contained elements, this is referred to as a Zr-U-O phase in cross-section observations for the sake of convenience.

Block [A-1] : JAEA Oarai

Overall SEM image of fragment



Measured with the sample affixed to carbon tape without vapor deposition

Zr-U-O phase and micro-mixed phases in the vicinity

Point 1
U, Fe, Ni, O

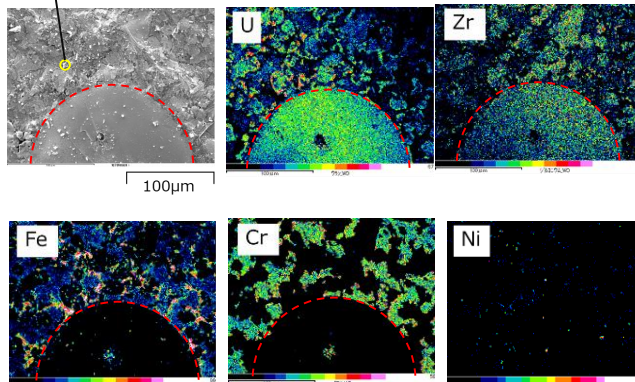


Figure 1 SEM image and element mapping

- There are regions of mixed microphases comprised of particles ranging in size from several μm ~several tens μm that contain U, Zr, Fe and Cr in the vicinity of phases approximately 200 μm in size (dashed lines in Figure 1) that contain high concentrations of U and Zr.
- Small amount of Ni exists (Figures 1 and 2)

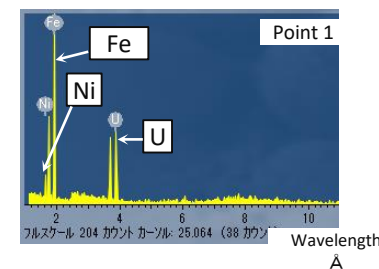


Figure 2 WDX point analysis spectrum that includes Ni

Fe-Ni(-O) phase (particles)

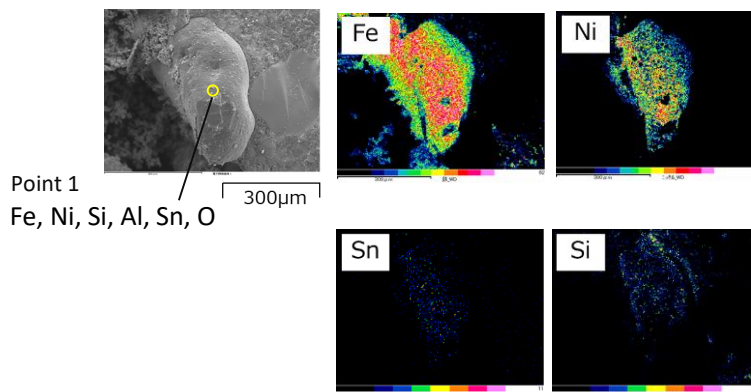


Figure 3 SEM image and element mapping

- Large particles approximately 300~400 μm in size that contain high concentrations of Fe and Ni exist. (Figure 3)
- Small amounts of Sn, Si and Al also exist. (Figure 4)

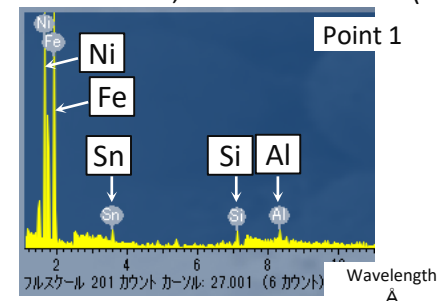
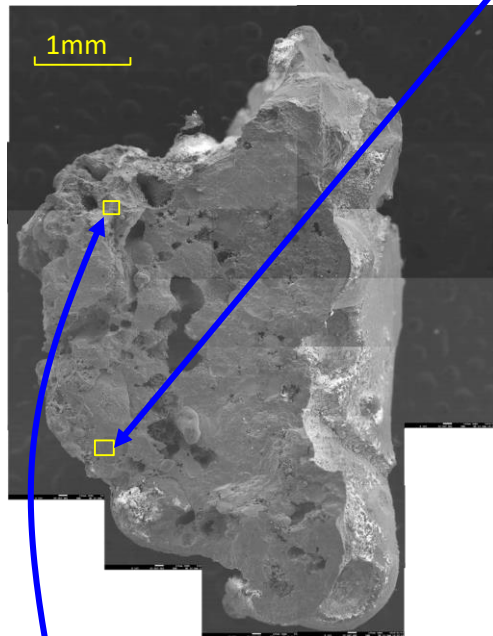


Figure 4 Granular WDX point analysis spectrum

Block【A-1】 : JAEA Oarai

Overall SEM image of fragment



Measured with the sample affixed to carbon tape without vapor deposition

Micro-mixed phase (1)

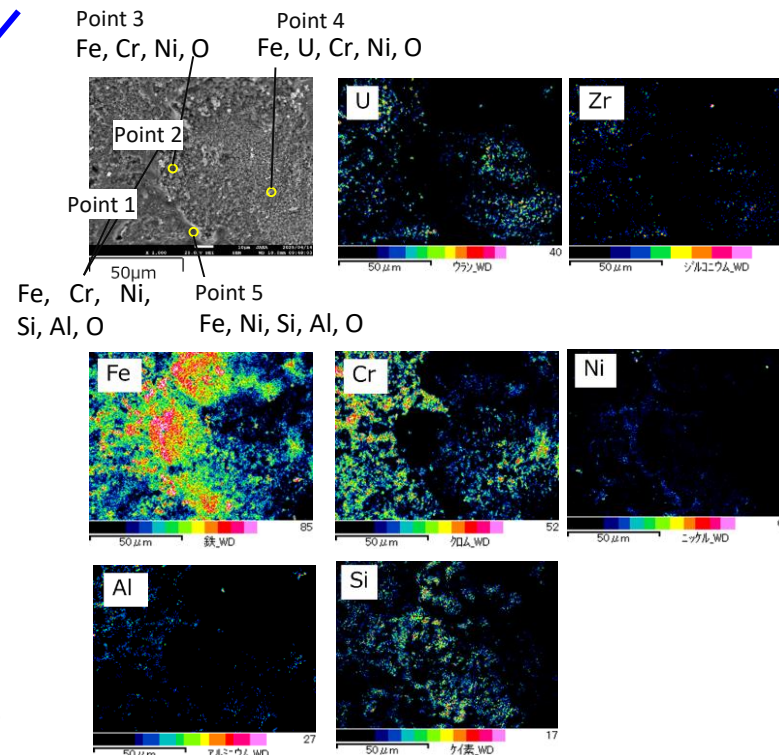


Figure 1 SEM image and element mapping

- Densely packed micro-phases 1~10μm in size exist. They consists primarily of U, Zr, Fe, Cr and Ni. (Figure 1)
- Small amounts of Al and Si were also detected. (Figure 2)

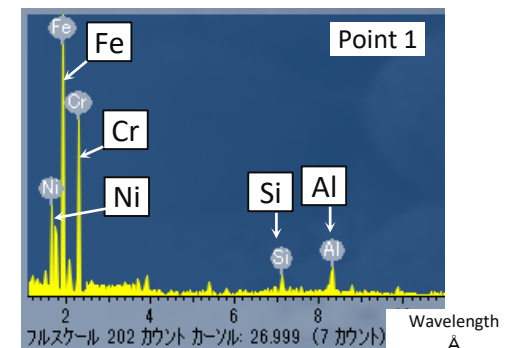


Figure 2 WDX point analysis spectrum of micro-mixed phases

Micro-mixed phase (2)

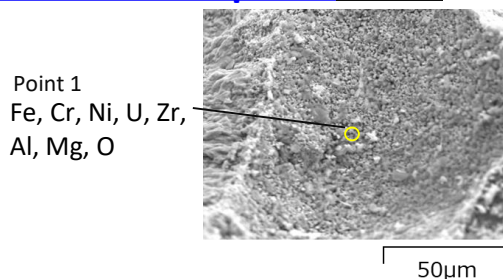
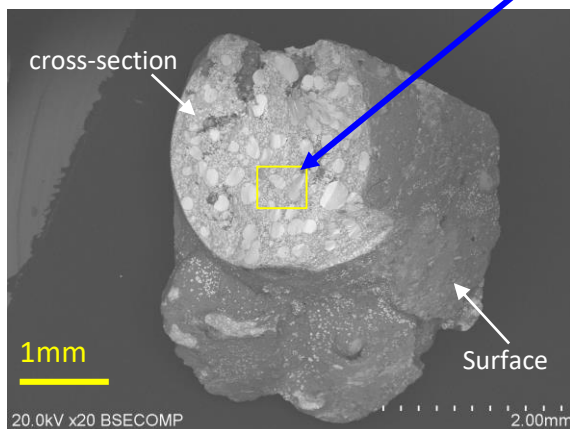


Figure 3 WDX point analysis spectrum and SEM images of micro-mixed phases

- Densely packed micro-phases 1~10μm in size exist just like in 1 (Figures 1 and 2). A very small amount of Mg exists. (Figure 3)

Block [D] : NDC

Overall SEM image of fragment



Measured with the sample affixed to carbon tape without vapor deposition



Zr-U-O phase and surrounding micro-mixed phases

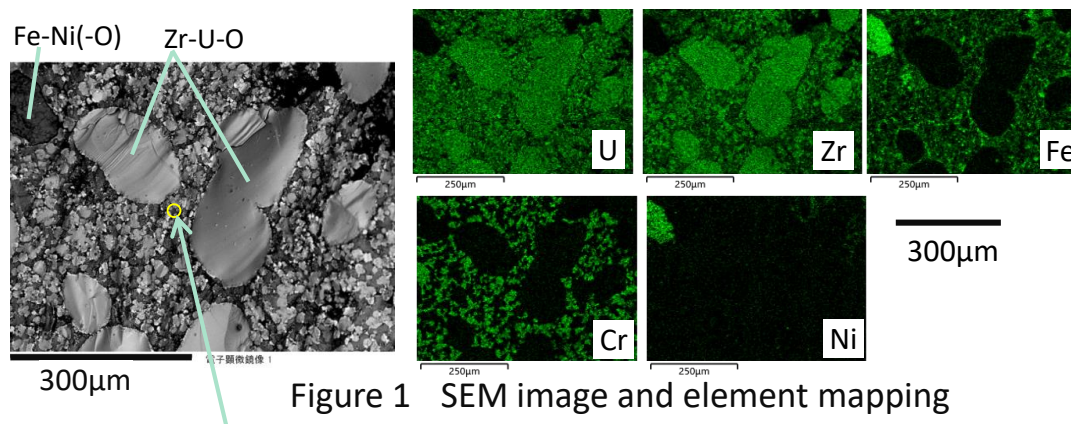


Figure 1 SEM image and element mapping

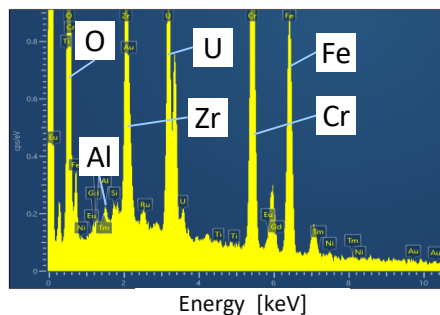
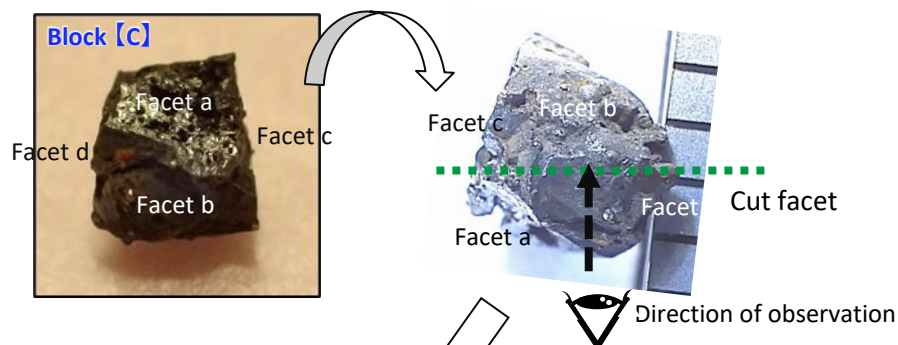


Figure 2 EDX point analysis spectrum of micro-mixed

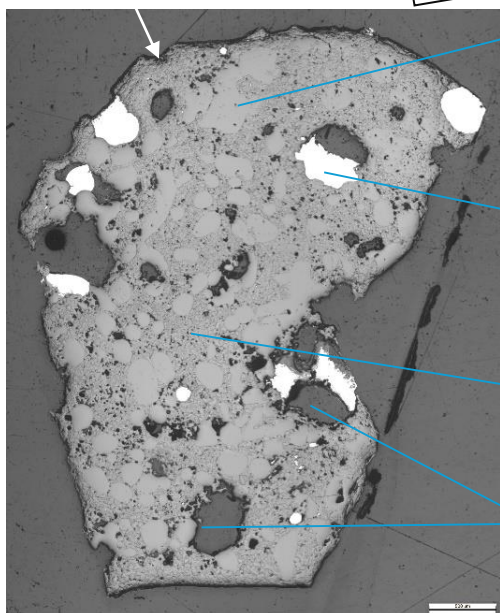
- There are regions where micro-phases (size: several μm to several tens μm) composed of U, Zr, Fe and Cr exist around phases several $10\sim 200\ \mu\text{m}$ containing high concentrations of U and Zr. (Figure 1)
- Small amounts of Al were also detected in the micro-mixed phases (Figure 2)

Block [C] : NFD

- Block [C] was cut and an image of the cross-section was obtained (Figure 1) to match with the x-ray CT image after which dose rates and micro-phase structure were assessed.
- Estimates of the porosity and the composition ratios of each region were assessed from analyzing the image of the cross-section. (figure 2)



Facet b outline



Optical microscope image

(A)Zr-U-O phase (several tens ~ several hundreds μm)

- The ratio of Zr/U was approx. 2
(Almost consistent regardless of particle)
- Also includes small amounts of Fe, Cr, and Ni

(B)Fe-Ni metal phase (several ~ several hundreds μm)

- Fe/Ni ration was approx. 1~3
(Differs depending on particle)

(C)Micro-mixed phase

- U-Zr-O, Zr-U-O, Fe-Cr-O, Fe-O mixed-phases

(D)Pore (several μm ~ several hundreds μm)

- Approx. 20% of the area of the cross-section



Image analysis example:
Assessment of void area ratio

Areas not red are
assumed to be
voids

(A) Zr-U-O	(B) Fe-Ni	(C) Micro phase	(D) Void
20	4.4	56	19

(A)Zr-U-O phase calculated as $100-(B)-(C)-(D)$

Figure 2 Area ratio assessment results for each region [%]

Going forward CT scans of these four regions will be taken in order to examine the ratios of the phases throughout the entire fuel debris sample.

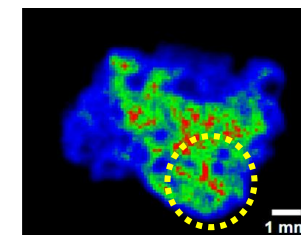


Figure 1 observations of the cut facets and cross-section of the fuel debris

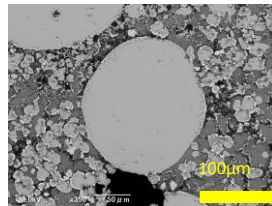
— Cross-section observations/composition assessment —

Block [C] : NFD

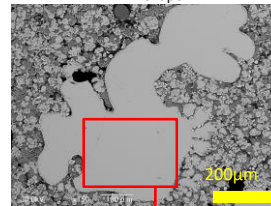
- Based on information about the microstructures and composition of each phase, we are hypothesizing the process by which the molten body became solid to ascertain the origins of the sample.

(A) Zr-U-O phase (several tens ~ several hundreds μm)

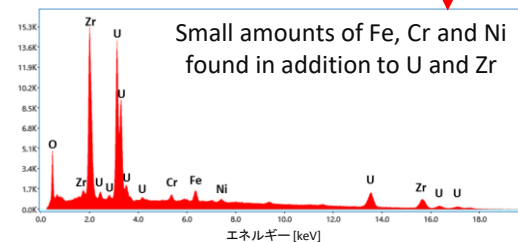
Example of rounded shape



Example of amorphous shape

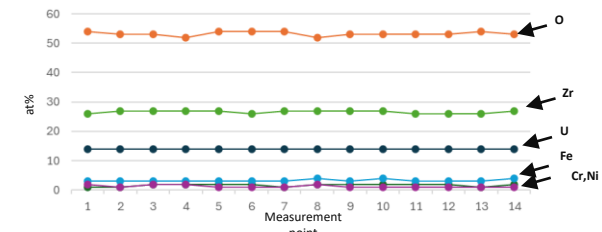


Zr-U-O phaseのSEM image



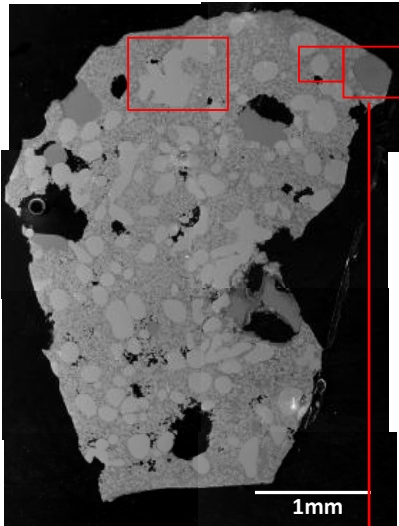
Zr-U-O phase facet analysis spectrum

- In addition to rounded shapes approximately $200\mu\text{m}$ in size, there are also amorphous phases that exceed $500\mu\text{m}$ in length.
 - In addition to Zr and U small amounts of Fe, Cr and Ni also exist, and there is almost no difference in composition between multiple phases.
- ⇒ It is hypothesized that molten U-Zr-Fe-Cr-Ni-O material dispersed and precipitated/grew in regions of the same temperature.



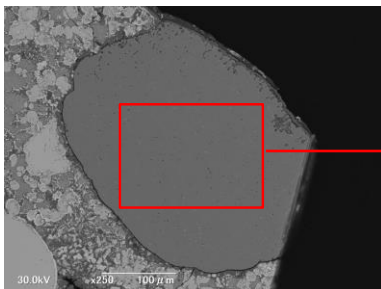
Note) Measurements 1~14 are point analysis results near the center of each different Zr-U-O phase
Shown as the total of O, Cr, Fe, Ni, Zr, and U being 100at%

Breakdown of major elements in the Zr-U-O phase

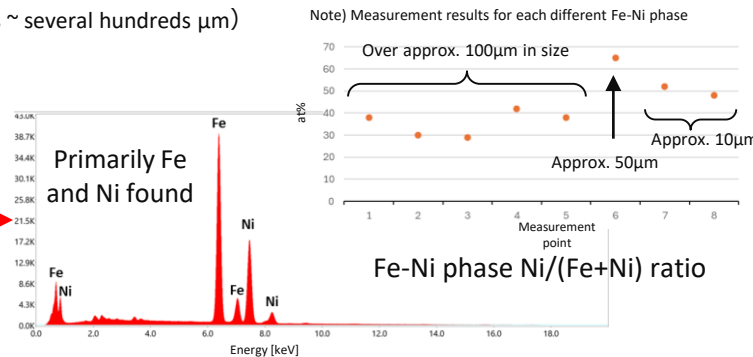


SEM image of whole specimen (BSE image)

(B) Fe-Ni metal phase (several tens ~ several hundreds μm)



Fe-Ni phase SEM image



Fe-Ni phase facet spectrum analysis

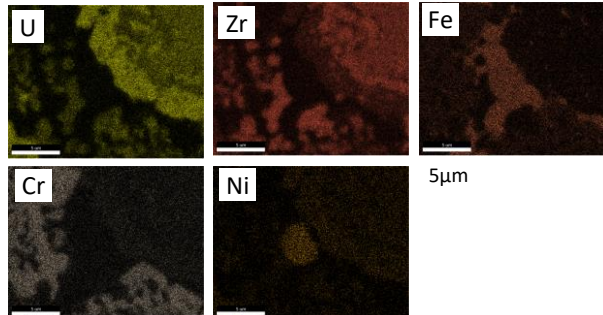
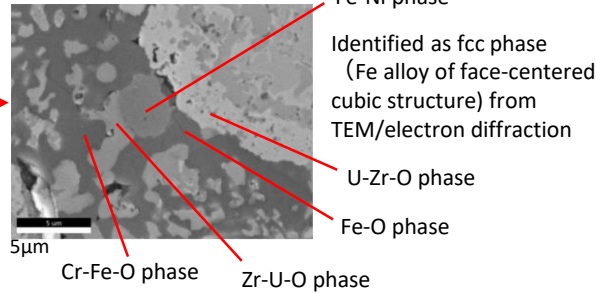
- Composed of primarily Fe and Ni. Most particles are over $100\mu\text{m}$ in size.
 - The Fe/Ni atomic ratio of phases that exceed approx. $100\mu\text{m}$ in size is around approx. 2, and no remarkable difference were found between measurement points.
- ⇒ It is hypothesized that molten Fe-Ni metal material existed separate from oxidized molten material.

— Cross-section observations/composition assessment —

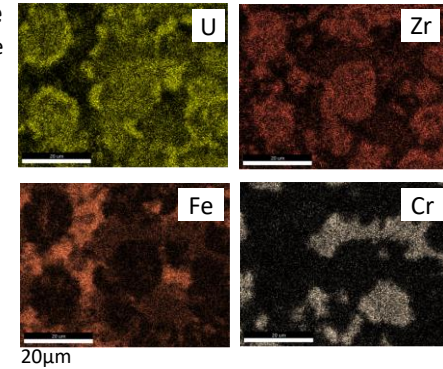
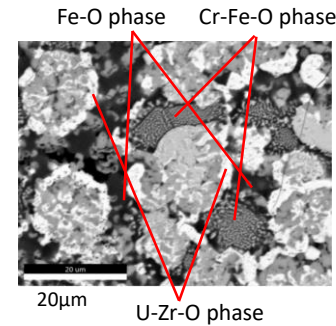
Block [C] : NFD

(C)Micro-mixed phase

Example of the inclusion of microscopic Fe-Ni metal phases

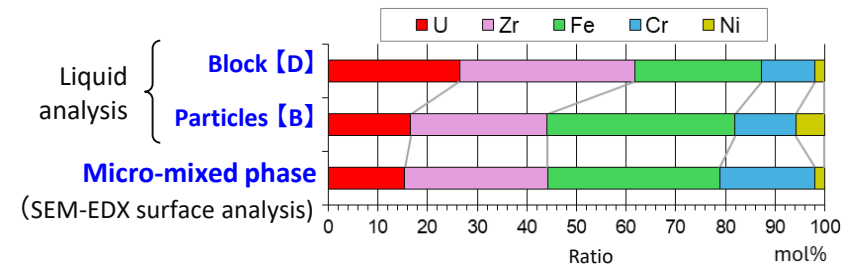


Example of microscopic oxide phase

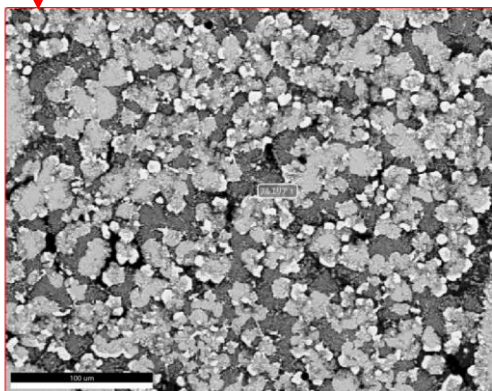


- U-Zr-O phases, Cr-Fe-O phases, and Fe-O phases found mixed into micro-mixed phases in addition to small (~several μm) phases of Zr-U-O and Fe-Ni.

⇒ It is hypothesized that precipitation of the Zr-U-O phase continued and turned into molten oxide material with high concentrations of Fe and Cr, after which each phase split apart, cooled, and solidified.



- The U:Zr:Fe:Cr:Ni ratio of the micro-mixed phase is close to the composition of particles [B] obtained through pulverization, indicating the possibility that powder was easily obtained through crushing.



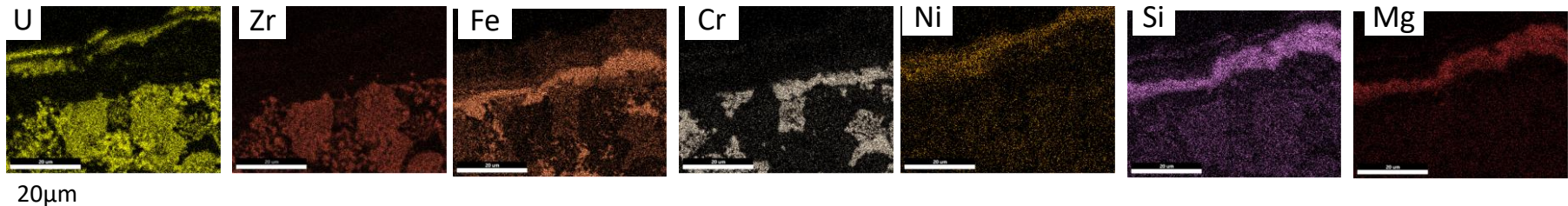
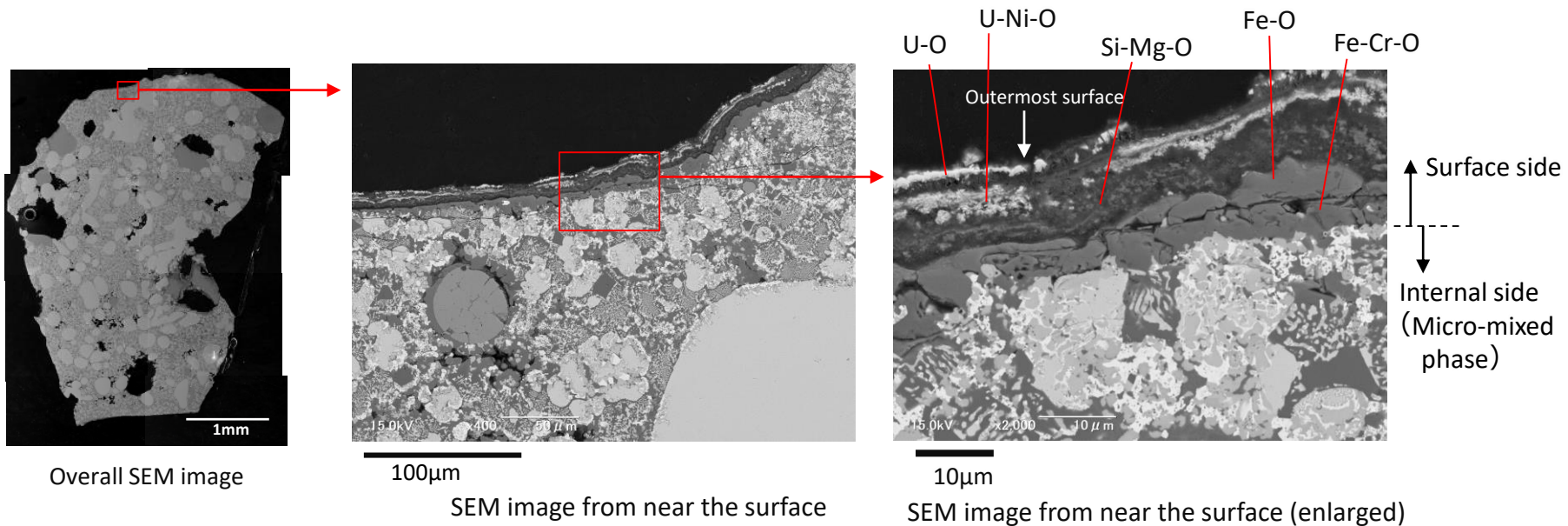
at%	
Major elements	Facet analysis
O	48
Cr	10
Fe	18
Ni	1
Zr	15
U	8

SEM-EDX facet analysis results of micro-mixed phase

Block [C] : NFD

(Reference) Structure near the surface

- Layers of U-O, U-Ni-O, Si-Mg-O, Fe-O, and Fe-Cr-O with structures that differ from the Zr-U-O phase, Fe-Ni metal phase, and micro-mixed phases, etc. found within have been deposited near the surface of the sample.



Map of primary elements near the surface (SEM-EDX mapping of enlarged area)

SEM observation image and map of primary elements near the surface

Particles [A-2] : JAEA Oarai

- Particles comprised mainly of U-Zr-Fe-Cr-Ni-O in powder [A-2] (Figure 1) obtained from crushing were focused on to contribute to hypotheses about the fuel debris creation process, and regions with unique external appearances and elemental distributions were subjected to SIMS and TEM localized analysis.

○ SIMS microscopic element distribution and changes in uranium isotope ratios

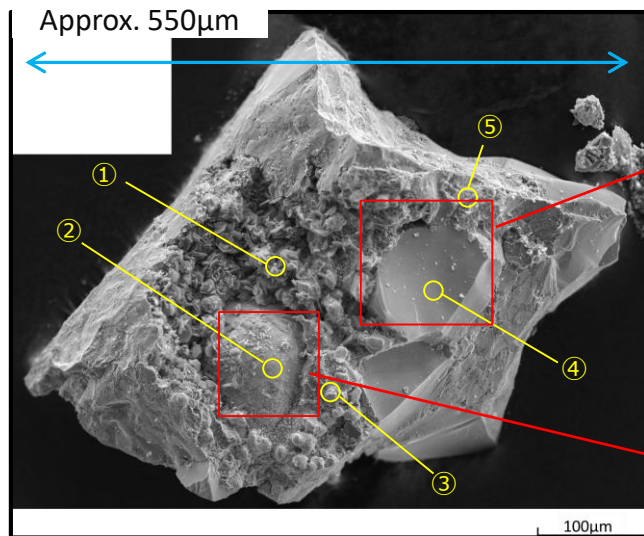


Figure 1 SIMS measurement locations on exterior of particle (①～⑤ indicate U isotope ratio measurement locations)

- Element distribution: Distribution of boron (B), which is difficult to detect through SEM-WDX, was confirmed (figure 2C dotted line). The composition and crystalline structure of phases containing B are being assessed using TEM.
- Localized uranium isotope ratio changes: It was confirmed that in the selected five locations (figure 1①～⑤), the peak count ratios of ^{235}U and ^{238}U were almost constant. It is assumed that even microscopically there are no remarkable discrepancies between uranium isotope ratios.

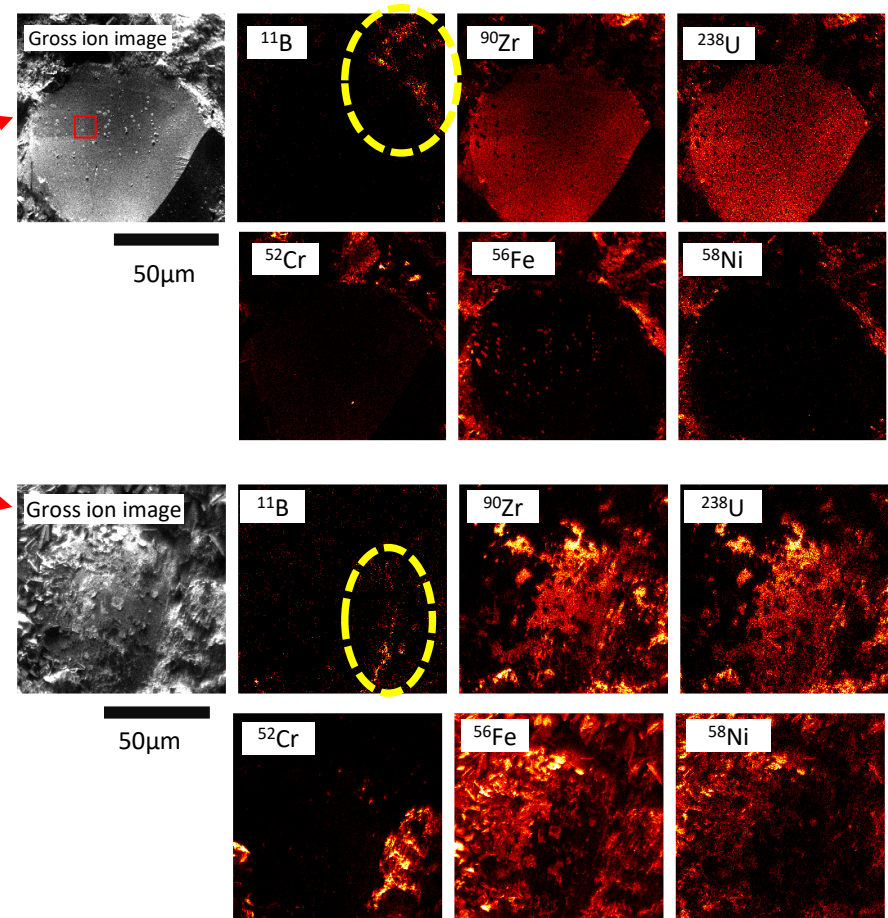
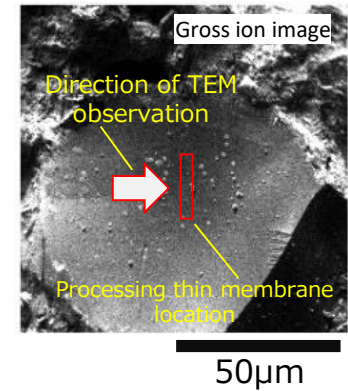


Figure 2 Results of element mapping using SIMS

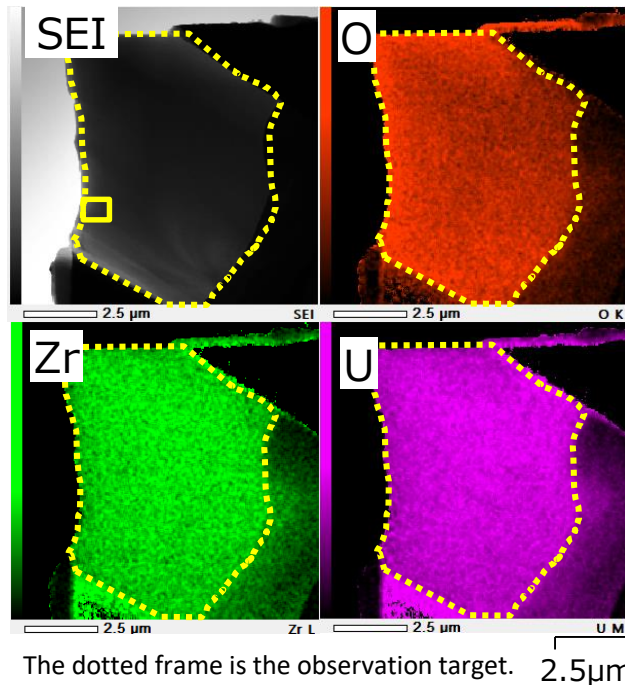
Particles [A-2] : JAEA Oarai

○ Crystalline structure assessment using TEM

- A thin membrane was made from the Zr-U-O phase found in the particles and subjected to TEM observation. (figure on the right)
- The electron diffraction pattern confirmed that this phase is composed of cubic crystal structures. (Refer to the figures below)



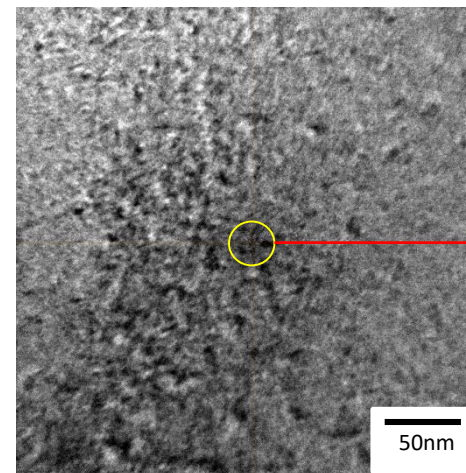
TEM observation location



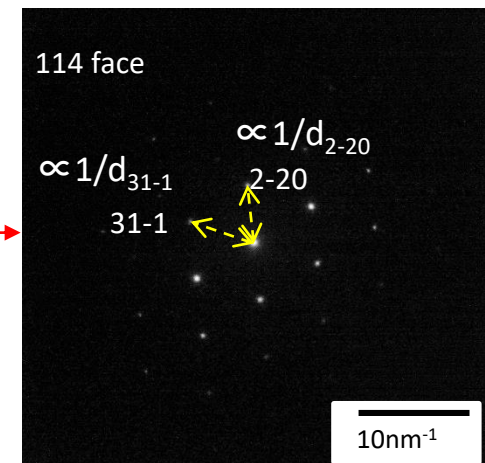
TEM observation image and major element distribution from a cross-section of the thin membrane that was prepared (TEM-EDX mapping)

$$d_{2-20} = 1.88 \text{ \AA} \quad ((\text{U,Zr})\text{O}_2 \text{ Theoretical value} : 1.88 \text{ \AA})$$

$$d_{31-1} = 1.61 \text{ \AA} \quad ((\text{U,Zr})\text{O}_2 \text{ Theoretical value} : 1.61 \text{ \AA})$$



TEM observation image (enlarged)



Electron diffraction pattern

Particles [A-2] : SPring-8

- Fragments created during the crushing of the fuel debris (specimen fragments approximately 0.1~1 mm in size (refer to figure 1)) were comprised of primarily of U, Zr, Fe and Ni, etc., and the chemical state of Pu, etc., was assessed.

<Procedure>

- Ascertaining the attributes of the entire specimen fragment:

First, the specimen was irradiated with a 2mm square synchrotron radiation x-ray to obtain an x-ray image of the entire specimen. Comprising elements, crystalline structure and the chemical state of each element were also examined through XRS, XRD and XAFS measurements. (Refer to the next page)

- Ascertaining the distribution in microscopic regions:

Concentrated synchrotron radiation x-rays were focused on a point of the specimen 1 μm in diameter to examine the comprising elements, crystalline structure and the chemical state distribution of microscopic regions using $\mu\text{-XRF}$, $\mu\text{-XRD}$ and $\mu\text{-XAFS}$. (Refer to the following pages and Figure 2)

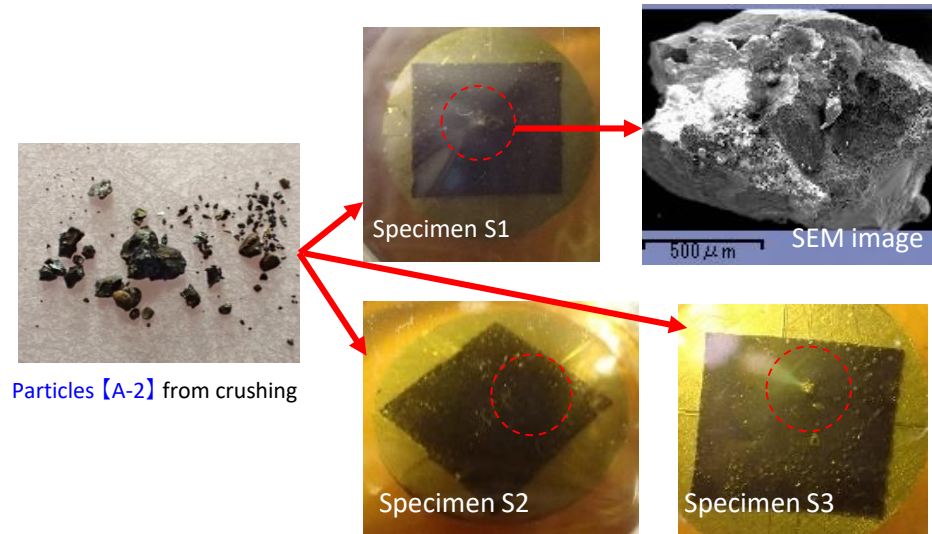


Figure 1 Created from three sealed specimens (Total mass: Approx. 3mg)

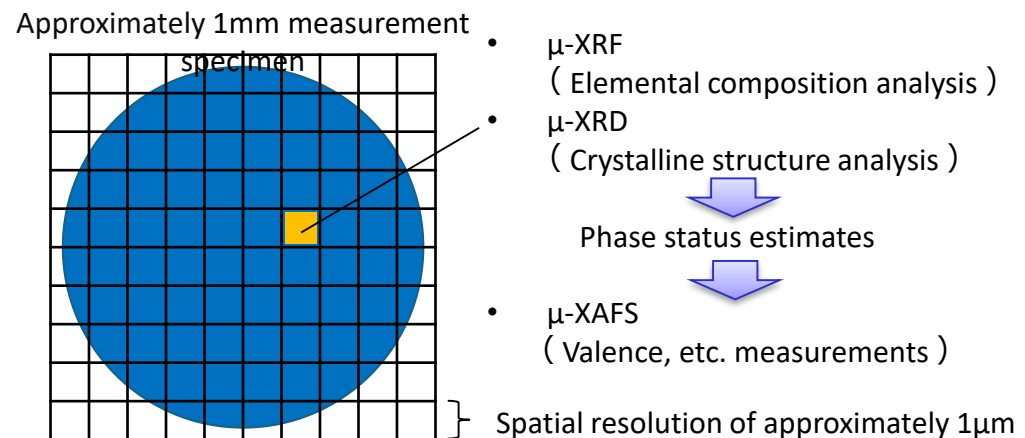


Figure 2 Measurement image using microbeams (1 μm square)

— Chemical state assessment of U, etc. from synchrotron analysis —

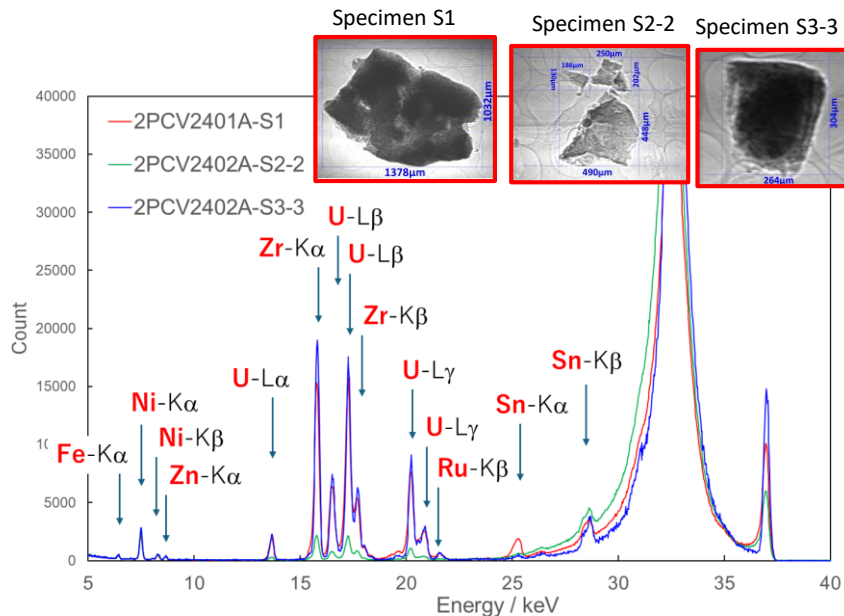
Particles【A-2】 : SPring-8

○ Element composition of each specimen fragment (2mm square XRF beam)

- The elemental composition of the entirety of the specimen fragment is a mixture of specimen fragments that contain U and Zr (U-rich) and specimen fragments that contain a lot of Fe, Ni and platinum group elements, but hardly any U (U-poor).

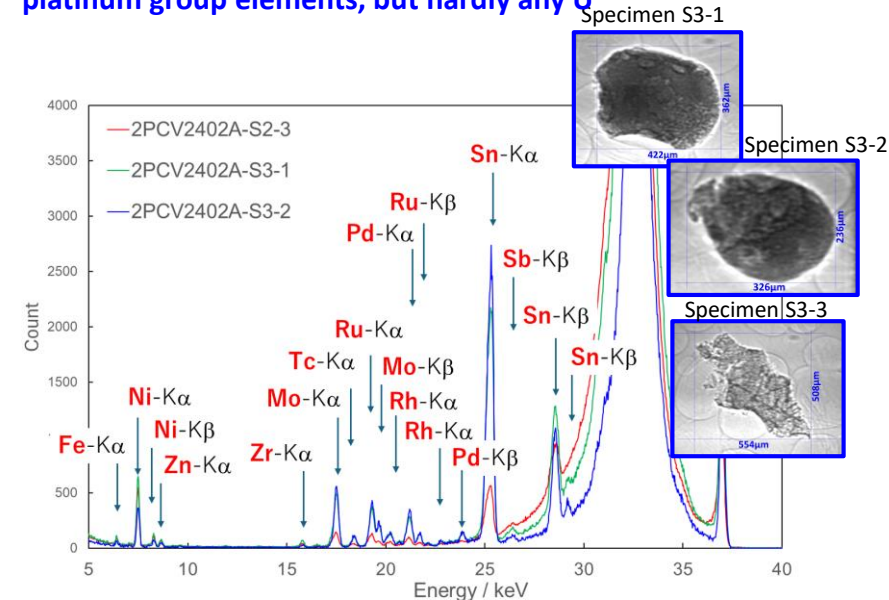
⇒ Is assumed that there are discrepancies in composition between regions approximately several hundred micrometers in size, which is the size of each specimen fragment.

U-rich : Specimen fragments that contain much U and Zr



Primarily U, Zr, Fe, and Ni. Includes small amounts of Ru and Sn.

U-poor : Specimen fragments that contain a lot of Fe, Ni and platinum group elements, but hardly any U



Primarily Sn, Pd, Rh, Ru, Tc, Mo, Ni, and Fe. Small amounts of Zr. Almost no U.

Particles [A-2] : SPring-8

○ Chemical state analysis of U and Pu

- U and Zr are distributed across the entirety of U-rich specimen fragments, with uneven distribution of Fe and Ni. μ -XAFS measurements were taken of multiple areas in which the major detected elements differ. (Refer to page 1~ page 8)
- The results from analyzing U and Pu valence in each measurement location by comparing the XAFS spectrums in existing literature^[1] with standard specimens that contain known valences were used to identify primarily quadrivalents. (Figure 2)
- Since XRD results from the entire specimen fragment (Figure 3) identified cubic crystals and tetragonal crystals containing U in addition to Fe_3O_4 phases, it is assumed that they exist primarily as dioxides.

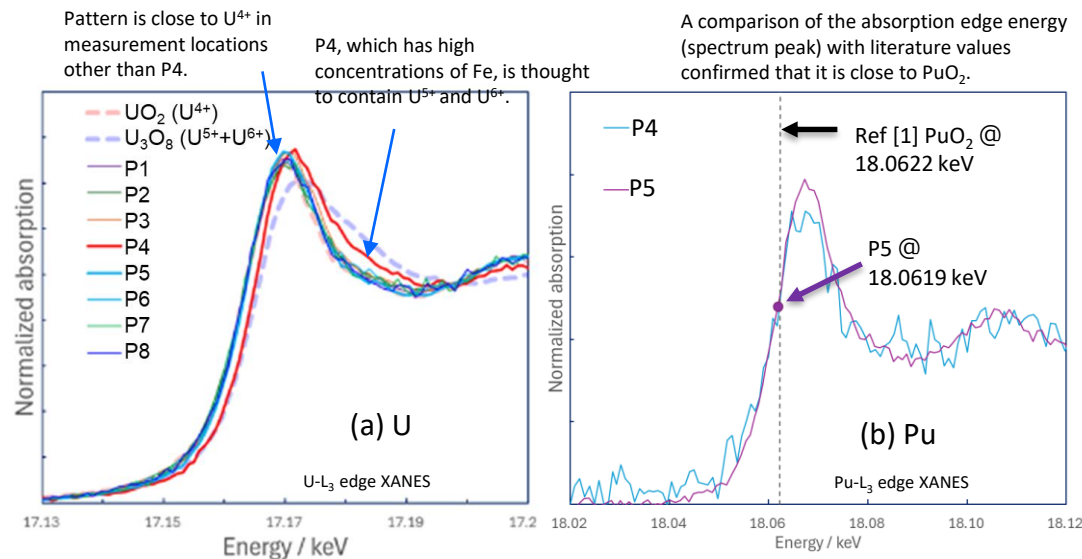
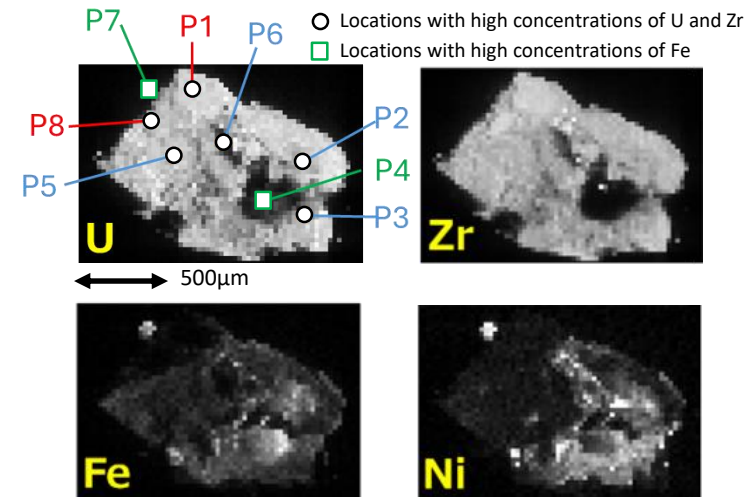


Figure 2 XAFS spectrum of U-rich specimen fragment [S1]



※ No significant CR signals were detected, and locations where it exists could not be identified

Figure 1 XRF mapping of U-rich specimen fragment [S1]

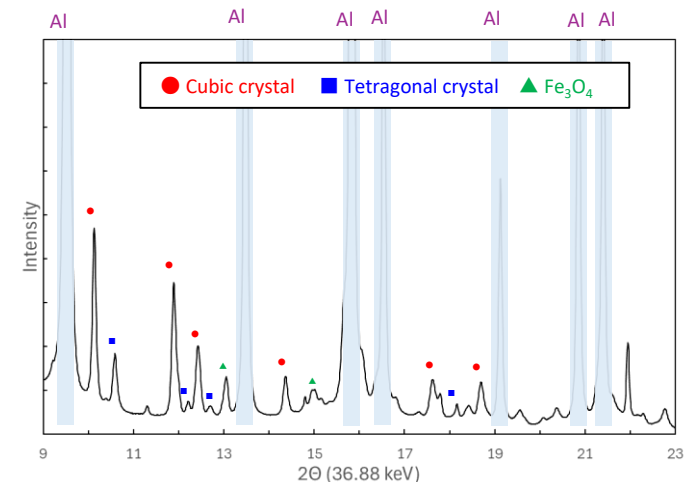


Figure 3 XRD of entirety of U-rich specimen fragment [S1]

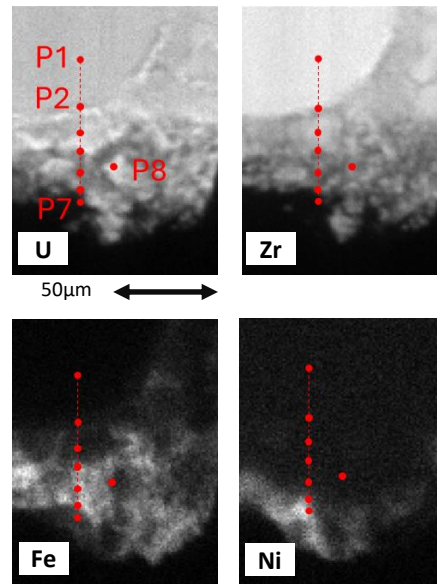
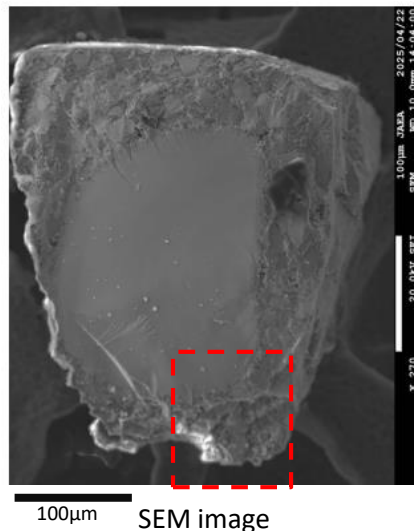
Particles [A-2] : SPring-8

○ Chemical state near the surface of the sample

- In some of the U-rich specimen fragments, the surface of the fuel debris was found to have layers of Ni. μ -XRF、 μ -XRD and μ -XAFS analysis using $1\mu\text{m}$ square synchrotron radiation targeting multiple measurement points near the surface was employed to examine differences in crystalline structure and chemical state between the inside and the surface of the sample. (Refer to the figures below)
- XAFS results showed a tendency for higher valences of uranium oxides near the surface. The results also indicated that Fe has oxidized on the surface.

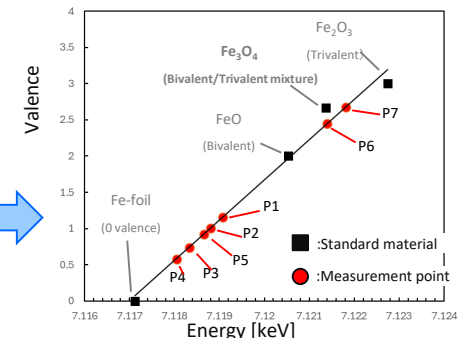
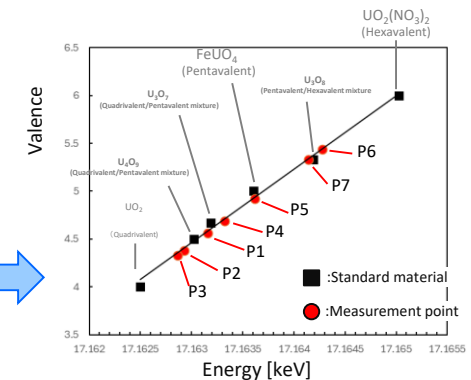
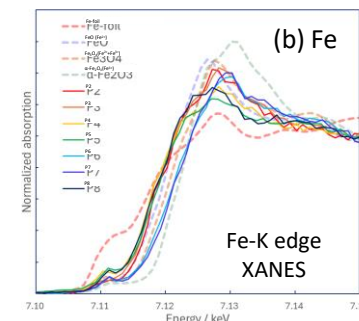
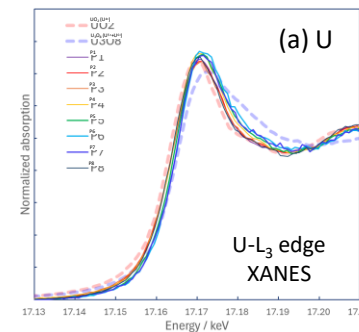
Valence was assessed by comparing the known standard materials with the adsorption edge locations (energy) of each measurement point

【Particle S3-3】



Element mapping (μ -XRF)
and μ -XAFS measurement locations

Obtained XAFS spectrum



μ -XAFS measurement results for each measurement location

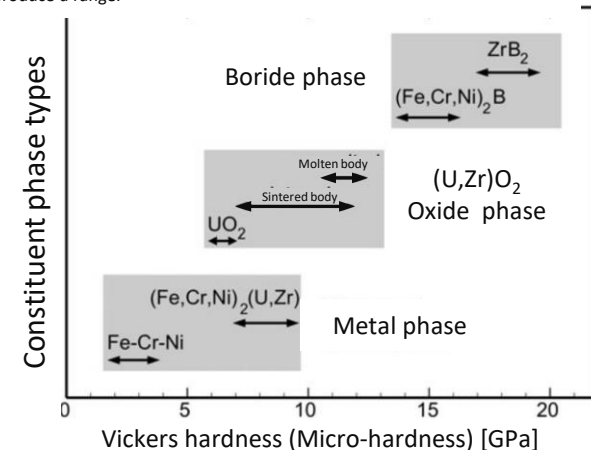
U and Fe valence assessment near the surface of the U-rich specimen fragment [S3]

- The hardness and toughness of constituent phases was estimated as shown below from the observed compound compositions.
- (Note) Estimates are not from actual measurements taken from the fuel debris sample, but rather from measurements taken from simulated fuel debris in the past.

Constituent phase (and size in sample)	Hardness ^{※1} [GPa]	Fracture toughness ^{※2} [MPa · m ^{1/2}]	Estimate summary
(A) Zr-U-O phase : Cubic crystal (Zr, U)O ₂ (Max. several 100μm in size)	≧Approx. 12	Approx. 1–2	※Refer to 3
(B) Fe-Ni metal phase : fcc-(Fe, Ni) (Max. several 100μm in size)	Approx. 1–4	~10 ²	※Refer to 4
(C) Micro-mixed phase : Mixed-phases Fe-Cr-O, Fe-O, etc. (Each phase being approximately 10μm in size maximum)	Approx. 5–15	Approx. 1–2	※Refer to 5

- ※1 **Hardness**: Index expressing the difficulty of an object to deform under stress. Materials with high hardness values tend to be more difficult to grind and cut. Vickers hardness is measured by pushing an indenter with a diamond tip (Vickers indenter) into the surface of the material and measuring the size of the indentation left behind. The chart above assumes that the measurements are taken at room temperature.
- ※2 **Fracture toughness**: Index expressing the energy required to generate a fissure. Materials with high fracture toughness values do not crack easily from shock. With oxidized materials it is common to make an indentation with a Vickers indenter and measure the length of the cracks around the indentation (indentation method). With metal materials, methods that differ from the indentation method, such as unloading tests and bending tests, etc. are often used. The chart above assumes that the measurements are taken at room temperature.
- ※3 **Zr-U-O phase hardness and toughness**: For cubic crystal phases with high Zr concentrations, the Vickers hardness of cubic crystal (Zr,U,Y)O₂ sintered bodies (Zr/(U+Zr)=65at%) from literature[1] and fracture toughness values from the indentation method (K_{IC} value) were referenced. The bottom limit for hardness has been listed in consideration of the fact that bodies that have melted and solidified tend^[2] to have higher values than sintered bodies.
- ※4 **Fe-Ni metal phase hardness and fracture toughness**: For hardness, the Vickers hardness range for Fe-Cr-Ni metal phases of specimens that have melted and then solidified (simulated fuel) found in literature [3] was referenced. Fracture toughness values were estimated from carbon steel and austenite stainless steel values in literature [4] [5] since it is difficult to measure the metal phases in a body that has melted and solidified. The order of toughness of these materials has been noted in consideration of fluctuations in composition and heat history based on a general range of 100~400MPa · m^{1/2} (K_{IC} value is constant)
- ※5 **Micro-mixed phase hardness and fracture toughness**: For hardness, the Vickers hardness of chromite (Mg and Al solidifies in FeCr₂O₄)^[6], magnetite (Fe₃O₄)^[7] and Fe-Cr oxide phases^[8] precipitated in specimens that have melted and solidified were referenced to produce a range. For fracture toughness, theoretical estimates for FeCr₂O₄, Fe₃O₄ and FeO were referenced to produce a range.

- Out of all the constituent phases generated through the melting and solidification of primary core materials, no large precipitated borides (see the figure to the right), which are one of the hardest phases, were found, and the amount of boron that exists in the sample was miniscule suggesting a minimal impact on mechanical properties.
- Since the hardness and fracture toughness of oxide phases and metal phases differ greatly, the content ratio and distribution of metal phases will be examined during the analysis of future fuel debris samples.



Vickers hardness^[3] of each constituent phase of the molten-solidified specimen (simulated)

[1] Kitagaki et al. J. Nucl. Eng. Rad. Sci., 4, 031011.

[2] For example, 2014 Revised Budget "Decommissioning/Contaminated Water Countermeasure Cost Subsidies (for ascertaining the nature of fuel debris)" FY2015 achievements report, April 2016.

[3] Takano et al., J. Nucl. Sci. Technol., 51, 859.

[5] Kasahara et al., JAEA-Review 2018-012.

[7] Takahashi et al., Iron and Steel 51, 1782.

[4] Iwadata et al., Materials 35 (395), 873.

[6] Bamba, Mining Geology, 33, 185.

[8] Tromans et al., Minerals Eng., 15, 1027.